

# Excitation spectra for Andreev billiards of Box and Disk geometries

J. Cserti, A. Bodor, J. Koltai and G. Vattay  
Eötvös University, Department of Physics of Complex Systems,  
H-1117 Budapest, Pázmány Péter sétány 1/A, Hungary

We study Andreev billiards of box and disk geometries by matching the wave functions at the interface of the normal and the superconducting region using the exact solutions of the Bogoliubov-de Gennes equation. The mismatch in the Fermi wavenumbers and the effective masses of the normal system and the superconductor, as well as the tunnel barrier at the interface are taken into account. A Weyl formula (for the smooth part of the counting function of the energy levels) is derived. The exact quantum mechanical calculations show equally spaced singularities in the density of states. Based on the Bohr-Sommerfeld quantization rule a semiclassical theory is proposed to understand these singularities. For disk geometries two kinds of states can be distinguished: states either contribute through whispering gallery modes or are Andreev states strongly coupled to the superconductor. Controlled by two relevant material parameters, three kinds of energy spectra exist in disk geometry. The first is dominated by Andreev reflections, the second, by normal reflections in an annular disk geometry. In the third case the coherence length is much larger than the radius of the superconducting region, and the spectrum is identical to that of a full disk geometry.

PACS numbers: 74.50.+r, 03.65.Sq

## I. INTRODUCTION

Recent technological advances in manufacturing almost ballistic semiconductors of mesoscopic size (two dimensional electron gas, 2DEG) coupled to a superconductor has initiated a growing interest in considering the phase-coherent transport and the excitation spectrum in hybrid superconducting nanostructures. In these systems the electron can coherently evolve into a hole (and vice versa) at the interface between the semiconductor and the superconductor. This mechanism had been discovered by Andreev<sup>1</sup>. Classically, the particle momentum is conserved and the hole is reflected back in the same direction as the incoming electron. This scattering process is known as retro-reflection or Andreev reflection. The overview of the recent progress in this field can be found in several works<sup>2-5</sup>. The Andreev scattering resulting in a discrete spectrum of single-particle excitations of a layer of normal metal in contact with superconductors on both sides was first discussed by Andreev<sup>1</sup>. Based on the Bogoliubov-de Gennes equation<sup>6</sup> (BdG) the excitation spectrum (Andreev states) of a normal metal (N) attached to a superconductor (S) was first considered by P. G. de Gennes and D. Saint-James<sup>7</sup>. A ballistic normal metal weakly coupled to a superconductor is commonly called an Andreev billiard. Such systems have been extensively studied over the past ten years<sup>8-15</sup>. The bound states were studied e.g. for SNS junctions<sup>16-18</sup>. A semi-infinite N region in contact with a semi-infinite S region in a strong magnetic field was investigated by Hoppe et al.<sup>19</sup>

The excitation spectrum of Andreev billiards depends on whether the N region is classically chaotic or integrable<sup>9,13-15</sup>. It has been shown that a gap opens in the spectrum for chaotic billiards, while for integrable billiards the spectrum is most likely to be gapless<sup>9</sup>. In these works the spectrum was calculated only close to the Fermi level. However, the spectrum shows interesting features throughout the entire energy range below the superconducting gap. The excitation spectrum is determined in this paper for two specific Andreev billiards, namely the NS box and disk systems. In NS box systems a rectangular N region is in contact with the superconductor, while the NS disk system consists of a circular S region surrounded concentrically by a circular N region. Both systems are integrable and, in accordance with earlier findings, the density of states (DOS) is gapless. We shall show, however, that for higher energies the DOS has singularities located at equal distances from each other.

One of the central issues in this paper is the investigation of these singularities in the DOS. We calculate the spectra of these systems exactly by solving the BdG equations, taking into account the non-perfect interface (mismatch in the Fermi wave numbers and the effective masses of the normal metal and the superconductor, and tunnel barrier at the interface). For a narrow NS junction it is justified<sup>2,3,5</sup> that the pairing potential can be approximated by a step-like function (zero in the N region and some constant value in the S region). Note that the two systems have the common feature that the BdG equation is separable and one of the separated wave function sets ('transverse modes') is the same in the N and the S region. The exact quantization condition can be very simply expressed in terms of a phase  $\Phi_m(\varepsilon)$  which is shown to be related to the classical action of an electron moving inside the N region between two successive bounces at the NS interface (see Eq. (26)).

Several authors<sup>9,10,13–15</sup> have already derived the Bohr-Sommerfeld approximation for the density of states. The DOS can be written in terms of the probability distribution  $P(s)$  of the classical path length  $s$  between two subsequent bounces of the electron at the NS interface. Starting from our exact quantization condition expressed in terms of the phase  $\Phi_m(\varepsilon)$  we re-derive the commonly used Bohr-Sommerfeld approximation<sup>9,14,15</sup> of the DOS in the case of NS box and disk systems. Moreover, we give an analytical expression for the probability  $P(s)$  in terms of the phase  $\Phi_m(\varepsilon)$ .

It is shown that, in the framework of Bohr-Sommerfeld quantization, the singularity of the DOS is a direct consequence of the singular behavior of  $P(s)$ . Using the expression for  $P(s)$  we can reproduce the counting function very accurately in the entire range of the spectrum and locate the singularities of the DOS for NS box and disk systems. The probability  $P(s)$  depends on the geometry of the N region and the location of the NS interface. We shall show that from a semiclassical point of view some special trajectories of the electron play crucial roles in the singular character of the DOS. Based on our semiclassical analysis a simple formula is given for the location of these singularities. This formula gives an excellent agreement with our numerically exact calculation of the spectrum. Furthermore, it predicts very accurately the number of the singularities and their location in the system studied by de Gennes et al.<sup>7</sup> We propose an explanation, based on our theory about the singularities, for the pronounced peaks found by Ihra et al.<sup>15</sup> (for NS systems) in their numerical calculations of the DOS. We believe that the singularities found by Lodder and Nazarov<sup>13</sup> (for Andreev billiards), and Šipr et al.<sup>20</sup> (for SNS systems) are related to some special classical trajectories of the electron for which the probability  $P(s)$  is singular.

The other issue studied in this paper is the Weyl formula for our NS systems. In the quantization of a normal billiard, the counting function  $N(E)$  gives the number of levels whose energy is less than or equal to  $E$ . The smooth part of the counting function  $N(E)$  is given by the Weyl formula<sup>21,22</sup>, which has already been calculated for billiards of various shapes. We present a new Weyl formula for our NS box and disk systems. As expected, the counting function obtained from the exact (numerical) calculations ‘oscillates’ around the curve given by our Weyl formula.

Our exact quantum mechanical results reveal a more complex energy level structure for NS disk systems than for box systems. Semiclassically, two kinds of modes exist in the disk geometry. First, the electron can hit the superconductor undergoing an Andreev reflection (hereafter called Andreev states), and second, the electron trajectory may not reach the superconductor (hereafter called whispering gallery modes). The two modes play crucial roles in the energy levels of the system. Contrary to NS box systems where the DOS is proportional to the energy close the Fermi level, in the case of NS disk systems it is constant due to the whispering gallery modes. In studying the spectrum of the disk geometry, we have been motivated by Bruder and Imry’s recent work<sup>23</sup>. Based on whispering gallery modes, they proposed a physical picture to interpret the significant paramagnetic effect observed in recent experiments<sup>24</sup>. Thus, a careful analysis of Andreev and whispering gallery states as presented in this paper and the inclusion of the flux induced phase may shed further light on the issue raised by Bruder and Imry<sup>23</sup>. Our work on this problem is in progress.

We also found that, depending on the parameters of the NS disk system, the spectra can belong to either of three classes: (a) ‘mixed phase’, in which Andreev states coexist with whispering gallery modes and the energy dependent coherence length  $\xi(\varepsilon)$  in the superconductor is much less than the radius  $R_S$  of the S region, while the DOS is singular; (b) the opposite case, i.e.  $\xi(\varepsilon) \gg R_S$  when the spectrum is identical to that of a normal billiard whose radius is that of the outer circle; (c) when  $k_F \xi(0)$  is order of one (here  $k_F$  is the Fermi wave number) or the NS interface is not perfect, and so the energy spectrum corresponds to that of an annular billiard (the circular S region is cut out). It turns out that there are two relevant parameters to make this classification,  $k_F \xi(\varepsilon)$  and  $k_F R_S$ . Using these parameters we sketch a so-called ‘phase diagram’ for the three above classes. It was reported in the works on the paramagnetic effect<sup>24</sup> that the coherence length exceeds the size of the superconducting region. Thus, according to our phase diagram it is possible that the whole NS disk system behaves as a full normal disk. Then a larger paramagnetic effect can be expected than that predicted by Bruder and Imry who included only the whispering gallery states. However, further work is necessary to clarify this scenario.

The text is organized as follows. In Sec. II a quantization condition (secular equation) is derived from the matching conditions of the wave functions at the interface of the NS systems. Owing to the symmetry of the BdG equation, the secular equation can be expressed in a very compact form valid both for NS box and disk systems. In Sec. III the Weyl formula is derived for NS box and disk systems and compared with the exact results. Our theory for the singularities in the DOS is presented in Sec. IV. We sketch the so-called ‘phase diagram’ for the NS disk systems in Sec. V, and the conclusions are given in Sec. VI.

## II. SECULAR EQUATION FOR BOX AND DISK

In this section we derive a secular equation determining the energy levels for box and disk geometries shown in Fig. 1. It is possible to treat both problems in a common framework by introducing the generalized coordinates

$$(x_1, x_2) = \begin{cases} (x, y), & \text{for box,} \\ (r, \varphi), & \text{for disk.} \end{cases} \quad (1)$$

The normal region is in contact with a superconducting region at  $x_1 = x_{\text{NS}}$  (where  $x_{\text{NS}} = 0$  for box and  $x_{\text{NS}} = R_S$  for disk).

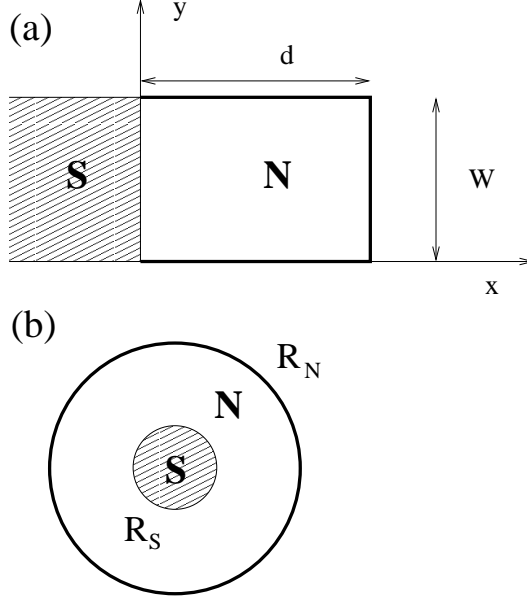


FIG. 1. The normal system (N) is in contact with the superconducting region (S). The two geometrical arrangements are (a) box geometry of side lengths  $d$  and  $W$  and (b) disk geometry (two concentric circles of radii  $R_S$  and  $R_N$ ). For the box, the generalized coordinates are  $(x_1, x_2) = (x, y)$ , while for the disk  $(x_1, x_2) = (r, \varphi)$  centered at the origin of the superconducting circle.

At the interface  $x_1 = x_{\text{NS}}$  the tunnel barrier is modeled by a Dirac delta potential  $V(x_1, x_2) = U_0 \delta(x_1 - x_{\text{NS}})$ , as in Ref. 25. The superconducting pairing potential is a constant  $\Delta_0$  in the S region and zero in the N region. The self-consistency of the pairing potential is not taken into account just like in Ref. 25. For a planar geometry the difference between the self-consistent gap and the step function is quite small as it was shown by McMillan and Kieselmann<sup>26</sup>. Similar results has been found by Plehn et al. in Ref. 27 for superconducting multilayers. For disk geometry the step function approximation is still reliable provided  $R_S$  is larger then the coherence length. However, the Fermi energies (i.e. the energy differences between the band edges of the N/S region and the chemical potential<sup>28</sup>) and the effective masses in the N and S regions are assumed to be different, i.e.  $E_F^{(N)} \neq E_F^{(S)}$  and  $m_N \neq m_S$ .

The NS system is described by the BdG equation:

$$\begin{pmatrix} H_0 & \Delta \\ \Delta^* & -H_0 \end{pmatrix} \Psi = \varepsilon \Psi, \quad (2)$$

where  $\Psi$  is a two-component wave function,  $H_0 = \mathbf{p}^2/2m - \mu$ , and the Fermi energy is  $\mu = E_F^{(N)}$  in the N region and  $\mu = E_F^{(S)}$  in the S region. The energy levels of the Andreev states are the positive eigenvalues  $\varepsilon$  of the Bogoliubov-de Gennes (BdG) equation<sup>6</sup>. In what follows, we consider the energy spectrum below the superconducting gap,  $\varepsilon < \Delta_0$ . The two-component wave functions  $\Psi$  in the N and S regions can be chosen in the form

$$\Psi_m^{(N)}(x_1, x_2) = \begin{pmatrix} a_m^{(e)} \varphi_m^{(N,e)}(x_1) \\ a_m^{(h)} \varphi_m^{(N,h)}(x_1) \end{pmatrix} \chi_m(x_2), \quad (3)$$

$$\Psi_m^{(S)}(x_1, x_2) = \left[ c_m^{(e)} \begin{pmatrix} \gamma_e \\ 1 \end{pmatrix} \varphi_m^{(S,e)}(x_1) + c_m^{(h)} \begin{pmatrix} \gamma_h \\ 1 \end{pmatrix} \varphi_m^{(S,h)}(x_1) \right] \chi_m(x_2), \quad (4)$$

where the 'transverse' wave function of the  $m$ th mode is

$$\chi_m(x_2) = \begin{cases} \sqrt{2/W} \sin(m\pi y/W), & \text{for box,} \\ e^{im\varphi}, & \text{for disk.} \end{cases} \quad (5)$$

The 'transverse' wave functions in the N and S regions are the same, and it is possible to separate the variables  $x_1, x_2$  in the BdG equation, i.e.  $\chi_m(x_2)$  depends only on the coordinate  $x_2$ .

The wave function  $\varphi_m^{(N,e)}(x_1)$  is the electron-like component of the eigenspinor of the BdG equation in the N region. It satisfies the one-dimensional Schrödinger equation obtained by separating  $\chi_m(x_2)$  in the BdG equation:

$$\varphi_m^{(N,e)}(x_1) = \begin{cases} \sin k_m^{(e)}(d - x), & \text{for box,} \\ J_m(k_e r) - \frac{J_m(k_e R_N)}{Y_m(k_e R_N)} Y_m(k_e r), & \text{for disk,} \end{cases} \quad (6)$$

where the energy dependence of the wave number  $k_m^{(e)}(\varepsilon)$  for box and  $k_e(\varepsilon)$  for disk are given by

$$k_m^{(e)}(\varepsilon) = k_F^{(N)} \sqrt{1 + \varepsilon/E_F^{(N)} - (m\pi/k_F^{(N)}W)^2}, \quad \text{for box,} \quad (7)$$

$$k_e(\varepsilon) = k_F^{(N)} \sqrt{1 + \varepsilon/E_F^{(N)}}, \quad \text{for disk,} \quad (8)$$

$k_F^{(N)}$  and  $E_F^{(N)}$  are the Fermi wave number and the Fermi energy in the N region, respectively, while  $J_m(x)$  and  $Y_m(x)$  are the Bessel and Neumann functions of order  $m$ . As we shall see below it is convenient to use real wave functions for  $\varphi_m^{(N,e)}(x_1)$ . The wave functions have been chosen such that they satisfy the Dirichlet boundary conditions at  $x = d$  for box and  $r = R_N$  for disk. Due to the symmetry of the BdG equation the hole-like component of the eigenspinor of the BdG equation in the N region is

$$\varphi_m^{(N,h)}(\varepsilon, x_1) = \varphi_m^{(N,e)}(-\varepsilon, x_1), \quad (9)$$

where the explicit dependence of the energy  $\varepsilon$  in the wave functions is emphasized for clarity.

The wave function in the S region is

$$\varphi_m^{(S,e)}(\varepsilon, x_1) = \begin{cases} \exp(-iq_m^{(e)}x), & \text{for box,} \\ J_m(q_e r), & \text{for disk,} \end{cases} \quad (10)$$

where

$$q_m^{(e)}(\varepsilon) = k_F^{(S)} \sqrt{1 + \eta - (m\pi/k_F^{(S)}W)^2}, \quad \text{for box,} \quad (11)$$

$$q_e(\varepsilon) = k_F^{(S)} \sqrt{1 + \eta}, \quad \text{for disk,} \quad (12)$$

$k_F^{(S)}$  and  $E_F^{(S)}$  are the Fermi wave number and the Fermi energy in the S region, respectively, and

$$\eta = \sqrt{\varepsilon^2 - \Delta_0^2}/E_F^{(S)}. \quad (13)$$

Note that for box  $\varphi_m^{(S,e)}(x) \rightarrow 0$  as  $x \rightarrow -\infty$  satisfying the boundary condition at  $-\infty$ . On the other hand, only the Bessel function can be chosen for disks, since the Neumann function is singular at the origin. Again, owing to the symmetry of the BdG equation, the hole-like component of the BdG spinor in the S region is

$$\varphi_m^{(S,h)}(\varepsilon, x_1) = [\varphi_m^{(S,e)}(-\varepsilon, x_1)]^*. \quad (14)$$

Finally, in Eq. (4)

$$\gamma_e = \Delta_0/(\varepsilon - \sqrt{\varepsilon^2 - \Delta_0^2}), \quad (15)$$

$$\gamma_h = \gamma_e^*. \quad (16)$$

The coefficients  $a_m^{(e)}, a_m^{(h)}, c_m^{(e)}, c_m^{(h)}$  in Eqs. (3)-(4) are determined from the boundary conditions at the interface of the NS system (see, e.g., Ref. 28):

$$\begin{aligned} \Psi_m^{(N)} \Big|_{x_1=x_{\text{NS}}} &= \Psi_m^{(S)} \Big|_{x_1=x_{\text{NS}}}, \\ \frac{d}{dx_1} \left[ \Psi_m^{(N)} - \frac{m_N}{m_S} \Psi_m^{(S)} \right] \Big|_{x_1=x_{\text{NS}}} &= \frac{2m_N}{\hbar^2} U_0 \Psi_m^{(S)} \Big|_{x_1=x_{\text{NS}}}. \end{aligned} \quad (17)$$

The matching conditions yield the following secular equation for the eigenvalues  $\varepsilon$  of the NS system for fixed mode index  $m$ :

$$D_m^{(\text{NS})}(\varepsilon) = \begin{vmatrix} \varphi_m^{(N,e)} & 0 & \gamma_e \varphi_m^{(S,e)} & \gamma_h \varphi_m^{(S,h)} \\ 0 & \varphi_m^{(N,h)} & \varphi_m^{(S,e)} & \varphi_m^{(S,h)} \\ \left[ \varphi_m^{(N,e)} \right]' & 0 & \gamma_e \left( Z \varphi_m^{(S,e)} + \frac{m_N}{m_S} \left[ \varphi_m^{(S,e)} \right]' \right) & \gamma_h \left( Z \varphi_m^{(S,h)} + \frac{m_N}{m_S} \left[ \varphi_m^{(S,h)} \right]' \right) \\ 0 & \left[ \varphi_m^{(N,h)} \right]' & Z \varphi_m^{(S,e)} + \frac{m_N}{m_S} \left[ \varphi_m^{(S,e)} \right]' & Z \varphi_m^{(S,h)} + \frac{m_N}{m_S} \left[ \varphi_m^{(S,h)} \right]' \end{vmatrix} = 0, \quad (18)$$

where  $Z = (2m_N/\hbar^2) U_0$  is the normalized barrier strength, and the prime stands for the derivative with respect to  $x_1$ . All the functions are evaluated at  $x_1 = x_{\text{NS}}$ .

Using the fact that the wave functions  $\varphi_m^{(N,e)}$  given in Eq. (6) are real functions and the symmetry relations between the electron-like and hole-like component of the BdG eigenspinor given by Eqs. (9) and (14), the above determinant can be simplified. One can show that the secular equation reduces to

$$\text{Im} \left\{ \gamma_e D_m^{(e)}(\varepsilon) D_m^{(h)}(\varepsilon) \right\} = 0, \quad (19)$$

where

$$D_m^{(e)}(\varepsilon) = \begin{vmatrix} \varphi_m^{(N,e)} & \varphi_m^{(S,e)} \\ \left[ \varphi_m^{(N,e)} \right]' & Z \varphi_m^{(S,e)} + \frac{m_N}{m_S} \left[ \varphi_m^{(S,e)} \right]' \end{vmatrix} \quad (20)$$

is a 2x2 determinant, and  $D_m^{(h)}(\varepsilon) = \left[ D_m^{(e)}(-\varepsilon) \right]^*$ . The energy levels of the NS systems can be found by solving the secular equation (19) for  $\varepsilon$  at a given quantum number  $m$ . The secular equation (19) is exact in the sense that the usual Andreev approximation is not assumed<sup>2</sup>. The Andreev approximation is valid only for  $\Delta_0/E_F \ll 1$  and quasi-particles whose incident/reflected directions are approximately perpendicular to the interface<sup>2</sup>.

### A. Secular equation for box

To find the energy levels for a box we shall give an explicit form of the secular equation (19). Inserting the wave functions given in Eq. (6) into Eq. (20) we obtain

$$D_m^{(e)}(\varepsilon) = \sin k_m^{(e)} d \left( Z - i \frac{m_N}{m_S} q_m^{(e)} + k_m^{(e)} \cot k_m^{(e)} d \right). \quad (21)$$

Hence, the secular equation given in Eq. (19) becomes

$$\text{Im} \left\{ \gamma_e \left( Z - i \frac{m_N}{m_S} q_m^{(e)} + k_m^{(e)} \cot k_m^{(e)} d \right) \left( Z + i \frac{m_N}{m_S} q_m^{(h)} + k_m^{(h)} \cot k_m^{(h)} d \right) \right\} = 0, \quad (22)$$

where  $k_m^{(h)}(\varepsilon) = k_m^{(e)}(-\varepsilon)$  and  $q_m^{(h)}(\varepsilon) = \left[ q_m^{(e)}(-\varepsilon) \right]^*$  are the wave numbers of the hole-like quasi-particles in the N and S regions, respectively. For a given quantum number  $m$  the energy levels can be found by solving the secular equation. Note that the case  $\sin k_m^{(e)} d = 0$  corresponds to the secular equation of the entire box with Dirichlet boundary conditions. Thus, it cannot be zero for the NS system. Semiclassically, small wave numbers  $k_m^{(e)}$  and  $k_m^{(h)}$  in the N region correspond to quasi-particles incident at grazing angles on the NS interface. In this case the Andreev approximation is not valid<sup>2</sup>. However, the secular equation (22) is *still* exact for the energy levels for box geometry.

## B. Secular equation for disk

We now derive the explicit form of the secular equation for disk geometry. Inserting the wave functions given in Eq. (6) into Eq. (20) we obtain

$$D_m^{(e)}(\varepsilon) = \begin{vmatrix} J_m(k_e R_S) - \frac{J_m(k_e R_N)}{Y_m(k_e R_N)} Y_m(k_e R_S) & J_m(q_e R_S) \\ k_e \left[ J'_m(k_e R_S) - \frac{J'_m(k_e R_N)}{Y'_m(k_e R_N)} Y'_m(k_e R_S) \right] & Z J_m(q_e R_S) + \frac{m_N}{m_S} q_e J'_m(q_e R_S) \end{vmatrix}, \quad (23)$$

where the primes denote the derivatives of the Bessel functions with respect to their arguments. For a given angular momentum quantum number  $m$  the energy levels are the solutions of the secular equation given in Eq. (19).

## III. WEYL FORMULA FOR NS SYSTEMS

For normal systems the counting function  $N(E)$  is the number of states whose energy is less than or equal to  $E$ . The derivative of the counting function with respect to the energy is the density of states. The smooth part of the counting function  $\tilde{N}(E)$  for a cavity was first derived by Weyl<sup>21</sup> (for more details see Ref. 22). The leading term of  $\tilde{N}(E)$  is given by the integral of  $\Theta(E - H_{\text{cl}}(\mathbf{p}, \mathbf{r}))$  over the phase space divided by  $h^2$ , where  $\Theta$  is the Heaviside function and  $H_{\text{cl}}$  is the Hamiltonian of the corresponding classical system. In two dimensions, and excluding the factor 2 for the spin, the smooth part of counting function  $\tilde{N}(E)$  is given by

$$\tilde{N}(E) = \frac{1}{h^2} \int_{H_{\text{cl}}(\mathbf{p}, \mathbf{r}) \leq E} d^2 p d^2 r \Theta(E - H_{\text{cl}}(\mathbf{p}, \mathbf{r})). \quad (24)$$

For Andreev states of energy  $\varepsilon$  less than  $\Delta_0$  it is not possible to define the classical Hamiltonian  $H_{\text{cl}}$ , therefore the smooth part of the counting function  $\tilde{N}(\varepsilon)$  cannot be derived from Eq. (24). As an alternative method for calculating the DOS one may start from the secular equation<sup>29,30</sup>. In this section we derive a Weyl formula for the NS systems shown in Fig. 1 using the secular equation (19).

For a given quantum number  $m$  let us introduce the eigenphase  $\Phi_m(\varepsilon)$  for the NS system:

$$\left[ D_m^{(e)}(\varepsilon) \right]^* / D_m^{(e)}(\varepsilon) = e^{i\Phi_m(\varepsilon)}. \quad (25)$$

Here we have assumed that  $D_m^{(e)}(\varepsilon) \neq 0$ , and in the following it will also be supposed that  $D_m^{(h)}(\varepsilon) \neq 0$ . In Sec. V the case  $D_m^{(e)}(\varepsilon) D_m^{(h)}(\varepsilon) = 0$  will be discussed. It is also assumed that the eigenphases  $\Phi_m(\varepsilon)$  are all monotonic and increasing with  $\varepsilon$ . The secular equation (19) can be further simplified:

$$\Phi_m(\varepsilon) - \Phi_m(-\varepsilon) - 2 \arccos \frac{\varepsilon}{\Delta_0} = 2n\pi, \quad (26)$$

where  $n = 0, \pm 1, \pm 2, \dots$ . Equation (26) is a very simple quantization condition for the NS system. The solutions of this equation give the energy spectrum  $\varepsilon_{mn}$  below the gap. The above-given quantization condition is a convenient starting point to calculate the DOS and the smooth part of the counting function. However, for numerical purposes Eq. (19) may be more suitable. Using (26) the density of states  $\rho(\varepsilon) = \sum_{m=1}^{M(\varepsilon)} \sum_{n=-\infty}^{\infty} \delta(\varepsilon - \varepsilon_{mn})$  for the NS system becomes

$$\rho(\varepsilon) = \sum_{m=1}^{M(\varepsilon)} \left| \frac{dF_m(\varepsilon)}{d\varepsilon} \right| \sum_{n=-\infty}^{\infty} \delta(F_m(\varepsilon) - n), \quad (27)$$

where  $2\pi F_m(\varepsilon) = \Phi_m(\varepsilon) - \Phi_m(-\varepsilon) - 2 \arccos(\varepsilon/\Delta_0)$ , and  $M(\varepsilon)$  is the number of 'transverse modes' depending on  $\varepsilon$ . Since the  $\Phi_m(\varepsilon)$  are all monotonic and increasing with  $\varepsilon$ , the derivatives  $dF_m(\varepsilon)/d\varepsilon$  are positive, and so the modulus sign is superfluous in (27). Applying the Poisson summation formula<sup>31,22</sup> to the second sum one finds

$$\rho(\varepsilon) = \sum_{m=1}^{M(\varepsilon)} \frac{dF_m(\varepsilon)}{d\varepsilon} \left[ 1 + 2 \sum_{k=1}^{\infty} \cos(2\pi k F_m(\varepsilon)) \right]. \quad (28)$$

The DOS can be separated into two parts: the smooth part, i.e. the  $k = 0$  term, and the oscillating part, which comes from the terms  $k \geq 1$  in Eq. (28). Here we consider only the smooth part. Then the Weyl formula, i.e. the smooth part of the counting function for NS system can be obtained from  $\tilde{N}(\varepsilon) = \int_0^\varepsilon \rho(\varepsilon') d\varepsilon'$ , and one finds

$$\tilde{N}(\varepsilon) = \frac{1}{2\pi} \sum_{m=1}^{M(\varepsilon)} [\Phi_m(\varepsilon) - \Phi_m(-\varepsilon)] + M(\varepsilon) \left( \frac{1}{2} - \frac{1}{\pi} \arccos \frac{\varepsilon}{\Delta_0} \right). \quad (29)$$

This is our Weyl formula for the NS systems. A similar treatment has been mentioned by Schomerus and Beenakker<sup>14</sup> in deriving the Bohr-Sommerfeld approximation of the DOS for Andreev's billiards. The number of transverse modes  $M(\varepsilon)$  is a discontinuous function of  $\varepsilon$ , therefore in Eq. (29) the sum has to be replaced by an integral to get the smoothed version of the counting function<sup>30</sup>. One can see that the Weyl formula is expressed in terms of the eigenphases  $\Phi_m(\varepsilon)$  defined in Eq. (25). Note that our Weyl formula is only valid for those systems in which a common set of the 'transverse wave' functions can be separated from the wave functions of the N and S regions. Lifting this condition is a possible extension of this problem.

### A. Weyl formula for box (no mismatch)

We now consider the Weyl formula for a perfect interface, i.e. for  $r_k = 1$ ,  $r_v = 1$ ,  $Z = 0$ . For simplicity, in the case of a perfect interface we shall use the notation  $k_F = k_F^{(N)} = k_F^{(S)}$  and  $E_F = E_F^{(N)} = E_F^{(S)}$ . From Eqs. (20) and (25), and in Andreev approximation ( $\Delta_0/E_F \ll 1$ , i.e.  $k_m^{(e)} \approx q_m^{(e)}$  except when they appear in an exponent), one finds

$$\Phi_m(\varepsilon) = 2k_m^{(e)} d. \quad (30)$$

Thus, from Eq. (26) the quantization condition becomes

$$\left( k_m^{(e)} - k_m^{(h)} \right) d = n\pi + \arccos(\varepsilon/\Delta_0). \quad (31)$$

Note that this result can also be derived from the Bohr-Sommerfeld quantization rule. In fact,  $\hbar\Phi_m(\varepsilon)$  is the classical *action* for the electron moving along the  $x$  direction between the superconductor and the wall at  $x = d$ .

The exact counting function  $N(\varepsilon)$  obtained (numerically) from Eq. (19) and the Weyl formula given in Eq. (29) are plotted in Fig. 2. For parameters see the figure caption.

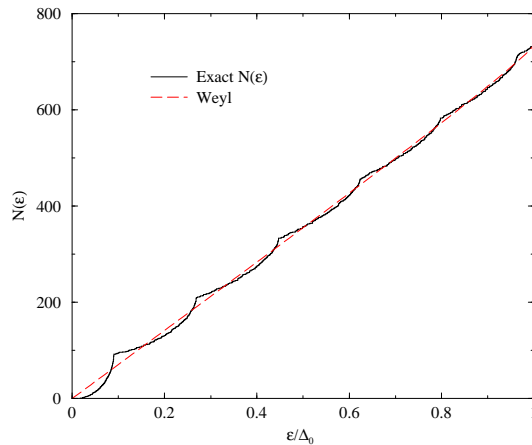


FIG. 2. The counting function  $N(\varepsilon)$  obtained from the exact quantum mechanical calculations (solid line) and the Weyl formula given in (29) (dashed line) as functions of  $\varepsilon/\Delta_0$  for the box geometry. The parameters are  $d/W = 3$ ,  $k_F W/\pi = 87.9$  and  $\Delta_0/E_F = 0.02$ .

One can see that the exact counting function oscillates around the curve obtained from our Weyl formula.

To find an analytical expression for the Weyl formula, the sum in Eq. (29) is replaced by an integral and we get

$$\tilde{N}(\varepsilon) = \frac{2}{\pi} \rho^{(N)} E_F g(\varepsilon/E_F) + M_h [1/2 - 1/\pi \arccos(\varepsilon/\Delta_0)], \quad (32)$$

where

$$g(x) = \sqrt{2x(1-x)} + (1+x) \arcsin \sqrt{(1-x)/(1+x)} - \pi/2(1-x), \quad (33)$$

and  $\rho^{(N)} = 2m/\hbar^2 A/(4\pi)$  is the density of states for the isolated N region of area  $A = Wd$ . The number of open channels for the hole-like quasiparticles is  $M_h = [k_F W/\pi \sqrt{1-\varepsilon/E_F}]$ , where  $[\dots]$  stands for the integer part. For  $x \ll 1$  (typically  $x < 0.1$ )  $g(x) \approx \pi x$ . Thus, the leading term of the smooth part of the counting function of Andreev states is  $\tilde{N}(\varepsilon) \approx 2\varepsilon \rho^{(N)}$ . Electron-like and hole-like quasiparticles make equal contributions to the Weyl formula (32), thereby the factor 2. The exact counting function  $N(\varepsilon)$  and the analytical form of the Weyl formula given in Eq. (32) are plotted in Fig. 3. It is seen from the figure that the analytical expression (dashed curve) deviates only for energies close to the gap.

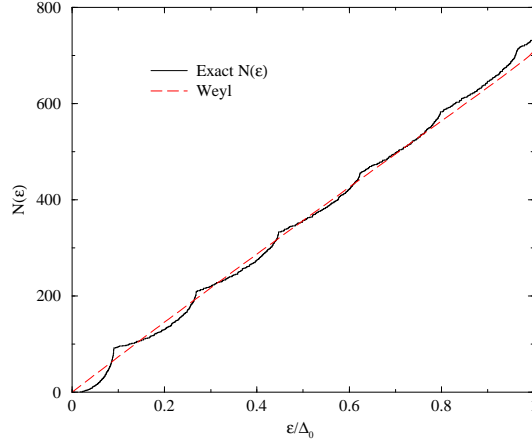


FIG. 3. The exact counting function  $N(\varepsilon)$  (solid line) and the analytical expression of the Weyl formula given in (32) (dashed line) as functions of  $\varepsilon/\Delta_0$  for the box geometry. The parameters are the same as in Fig. 2.

### B. Weyl formula for disk (no mismatch)

In this section an analytical expression of the Weyl formula is derived for disk geometry. However, most of the results obtained in this section will be used in Sec. IV B, too. Again, we shall take the case of perfect NS interface, namely no mismatch and tunnel barrier are assumed ( $r_k = 1$ ,  $r_v = 1$ ,  $Z = 0$ ). To find an analytical expression for the eigenphase  $\Phi_m(\varepsilon)$  defined in Eq. (25) we have to approximate the determinant  $D_m^{(e)}(\varepsilon)$  in (23). The details of the approximations are presented in Appendix A.

To summarize, according to the approximations of the determinants appearing in the secular equation (19), three ranges of  $m \geq 0$  can be distinguished: for Andreev states  $m < k_h R_S - \sqrt[3]{k_h R_S}$ , for whispering gallery states  $m > k_e R_S + \sqrt[3]{k_e R_S}$ , and for intermediate states  $k_h R_S - \sqrt[3]{k_h R_S} < m < k_e R_S + \sqrt[3]{k_e R_S}$ . Owing to the degeneracy of the  $\pm m$  states the three ranges for  $m \geq 0$  and  $m \leq 0$  are symmetrically located with respect to the state  $m = 0$ . This structure of the energy levels will be called a ‘mixed phase’ (MP). The exact energy levels,  $\varepsilon_{nm}$  obtained (numerically) from (19) are shown as functions of the angular quantum number  $m$  in Fig. 4. For each  $m$  the solutions are labeled by the quantum number  $n$  (radial quantum number). Since the pairs  $\pm m$  are degenerate, only  $m \geq 0$  states are plotted in the figure.



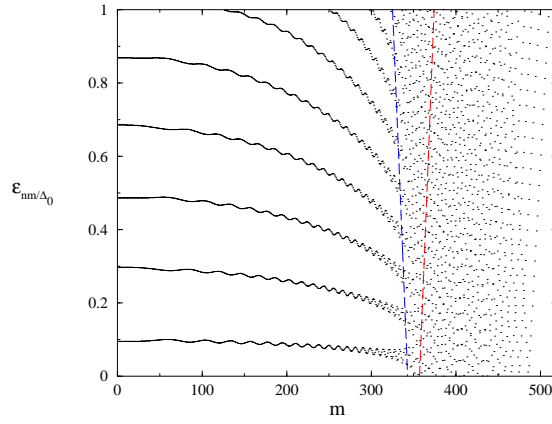


FIG. 4. The exact energy levels,  $\varepsilon_{nm}$  (dots) in units of  $\Delta_0$  as a function of the angular momentum quantum number  $m$ . There is no mismatch, and the potential of the tunnel barrier is zero. The parameters are  $R_S/R_N = 0.7$ ,  $\Delta_0/E_F = 0.1$ , and  $k_F R_S = 350$ . The intermediate  $m$  states are located between the two dashed lines. The Andreev states are to the left of the left dashed line, and the whispering gallery modes are to the right of the right one.

The two dashed lines in Fig. 4 separate the three types of states characterized by  $m$ . One can see that the intermediate states indeed occupy a narrow range in  $m$  compared to Andreev and whispering gallery states. It is also clear from the figure that the energy levels for Andreev states ‘oscillate’ with increasing amplitude as  $m$  increases towards the onset of the intermediate states (left dashed line in the figure). Inserting Eq. (A10) into the quantization condition given by Eq. (26) one can approximately calculate the energy levels for Andreev states. Plotting these energy levels in Fig. 4 (not shown in the figure) we found that the exact energy levels ‘oscillate’ around these approximate ones. Similar behavior of the energy levels has been found by Šipr et al.<sup>20</sup>. For whispering gallery states the approximate secular equation is given by Eq. (A11), and its solutions coincide very accurately with exact energy levels. These approximate energy levels for Andreev and whispering gallery states are those which can be obtained from the semiclassical quantization of the Schrödinger equation describing the radial motion of the electron<sup>22</sup>. Indeed, one can check that the first two terms for  $\Phi_m(\varepsilon)$  in Eq. (A9) multiplied by  $\hbar$  give the *radial action* for the electron moving between the two circles. The last three terms are constant, i.e. independent of  $\varepsilon$  therefore they do not play any role in the dynamics of electron. These trajectories of the electrons correspond to Andreev states. The semiclassical orbits for Andreev and whispering gallery states are shown in Fig. 5.

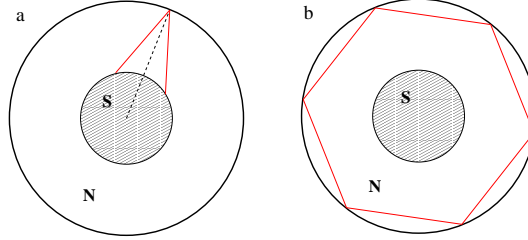


FIG. 5. The corresponding semiclassical orbits for (a) Andreev states and (b) whispering gallery states.

Inserting (A10) into the Weyl formula (29) one can determine the contributions of the Andreev states to the smooth part of the counting function:

$$\tilde{N}_{AS}(\varepsilon) = \frac{1}{\pi} \sum_{|m| < M_{AS}} [\vartheta_m(k_e R_N) - \vartheta_m(k_e R_S) - \vartheta_m(k_h R_N) + \vartheta_m(k_h R_S)] + 2 M_{AS} \left( \frac{1}{2} - \frac{1}{\pi} \arccos \frac{\varepsilon}{\Delta_0} \right), \quad (34)$$

where  $M_{AS} = \lfloor k_h R_S - \sqrt[3]{k_h R_S} \rfloor$  is the highest  $m$  for the Andreev states.

For whispering gallery modes the eigenphase  $\Phi_m(\varepsilon)$  in (25) cannot be determined because  $D_m^{(e)}(\varepsilon)$  is approximately zero. In this case the contribution to the smooth part of the counting function will be calculated from the secular equation (A11) for whispering gallery states. It is well known that the zeros of the Bessel functions can be determined to a good approximation by applying Debye’s asymptotic expansion given in Eq. (A1). The solution of the secular equation (A11) for whispering gallery states is then equivalent to the solution of the following pair of equations for  $\varepsilon$ :

$$F_m^{(e)}(\varepsilon) = \frac{1}{\pi} \vartheta_m(k_e R_N) - \frac{3}{4} = n_1 \quad (35)$$

$$F_m^{(h)}(\varepsilon) = \frac{1}{\pi} \vartheta_m(k_h R_N) - \frac{3}{4} = n_2, \quad (36)$$

where  $n_1, n_2 = 0, \pm 1, \pm 2, \dots$ , and  $\vartheta_m(x)$  is given by Eq. (A5). From these equations one can find the density of states of whispering gallery states much in the same way as from Eq. (27) for the Andreev states:

$$\rho_{\text{wgs}}(\varepsilon) = 2 \sum_{m=M_{\text{wgs}}}^{k_e R_N} \left| \frac{dF_m^{(e)}(\varepsilon)}{d\varepsilon} \right| + 2 \sum_{m=M_{\text{wgs}}}^{k_h R_N} \left| \frac{dF_m^{(h)}(\varepsilon)}{d\varepsilon} \right|, \quad (37)$$

where  $M_{\text{wgs}} = \lceil k_e R_S + \sqrt[3]{k_e R_S} \rceil$  is the smallest angular momentum quantum number  $m$  for whispering gallery states, and the factor 2 corresponds to the  $\pm m$  degeneracy. The contribution of whispering gallery states to the smooth part of the counting function can be obtained from  $\tilde{N}_{\text{wgs}}(\varepsilon) = \int_0^\varepsilon \rho_{\text{wgs}}(\varepsilon') d\varepsilon'$  which yields

$$\tilde{N}_{\text{wgs}}(\varepsilon) = \frac{2}{\pi} \sum_{m=M_{\text{wgs}}}^{k_e R_N} \vartheta_m(k_e R_N) - \frac{2}{\pi} \sum_{m=M_{\text{wgs}}}^{k_h R_N} \vartheta_m(k_h R_N). \quad (38)$$

The negative sign in front of the second term comes from the fact that the derivative of  $\vartheta_m(k_h R_N)$  with respect to  $\varepsilon$  is negative.

The counting function  $\tilde{N}(\varepsilon)$  for the NS disk system is the sum of the contribution of Andreev states ( $\tilde{N}_{\text{AS}}(\varepsilon)$ ) and that of whispering gallery states ( $\tilde{N}_{\text{wgs}}(\varepsilon)$ ). We now neglect the contribution of the intermediate states. To find an analytical expression for  $\tilde{N}(\varepsilon)$ , the summation over  $m$  is replaced by an integral in Eqs. (34) and (38) and for  $k_F R_S \gg 1$   $M_{\text{AS}} \approx M_{\text{wgs}} \approx k_h R_S$  is taken. The last approximation corresponds to replacing the intermediate states by whispering gallery states. This is quite a good approximation, since the number of intermediate states is much smaller than that of the Andreev and whispering gallery states. The resulting integrals can be performed analytically. After some algebra we obtain

$$\tilde{N}(\varepsilon) = \frac{k_F^2 R_N^2}{2} \frac{\varepsilon}{E_F} - \frac{k_F^2 R_S^2}{2} g\left(\frac{\varepsilon}{E_F}\right) + 2k_F R_S \sqrt{1 - \frac{\varepsilon}{E_F}} \left( \frac{1}{2} - \frac{1}{\pi} \arccos \frac{\varepsilon}{\Delta_0} \right), \quad (39)$$

where

$$g(x) = \frac{3}{\pi} \sqrt{2x(1-x)} + \frac{1}{\pi} (1+x) \arcsin \sqrt{\frac{1-x}{1+x}} - (1-x) \left( \frac{1}{2} + \frac{2}{\pi} \arccos \sqrt{\frac{1-x}{1+x}} \right). \quad (40)$$

This is our Weyl formula for NS concentric disk systems. Usually,  $\varepsilon/E_F \ll 1$  and for  $x \ll 1$ ,  $g(x) = x$  in leading order, therefore the first two terms in Eq. (39) yield  $2\rho^{(\text{N})}\varepsilon$ , where  $\rho^{(\text{N})} = 2m/\hbar^2 A/(4\pi)$  is the density of states for a normal annular billiard of area  $A = (R_N^2 - R_S^2)\pi$ . The factor 2 comes from the electron/hole contributions for NS systems. The higher order corrections in  $g(x)$  become more relevant with increasing  $\varepsilon$ . The last term in (39) is related to the phase shift due to the Andreev reflection at the NS interface. It is important to stress that the Weyl formula given in Eq. (39) was derived for the case  $R_S \gg \xi(\varepsilon)$ , i.e. when Andreev states and whispering gallery states coexist (mixed phase). In the opposite case, as we shall see in Sec. V, no Andreev states exist.

In Fig. 6 the exact counting function and the Weyl formula given by Eq. (39) are plotted as functions of  $\varepsilon/\Delta_0$ . For parameters see the figure caption.

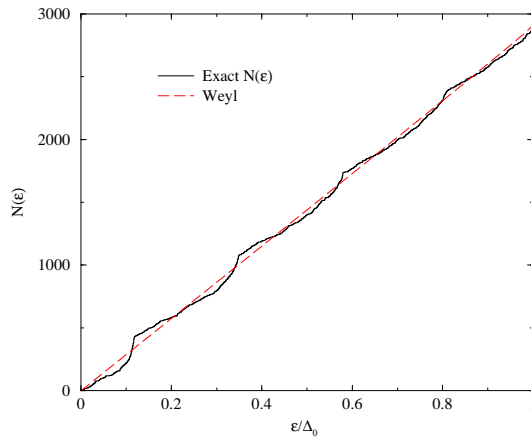


FIG. 6. The exact counting function  $N(\varepsilon)$  obtained from Eqs. (19) (solid line) and  $\tilde{N}(\varepsilon)$  given by (39) (dashed line) as functions of  $\varepsilon/\Delta_0$  for the disk geometry. There is no mismatch and the potential of the tunnel barrier is zero. The parameters are:  $R_S/R_N = 2/7$ ,  $\Delta_0/E_F = 0.05$  and  $k_F R_S = 100$ .

The singularities of the DOS (derivative of the counting function with respect to  $\varepsilon$ ) will be discussed in the next section.

#### IV. SINGULARITIES IN DOS

The exact counting function,  $N(\varepsilon)$  has *cusps* at some energies as shown Figs. 2 and 6 for box and disk geometries, and perfect interface. This implies that the DOS of the Andreev states is *discontinuous* here. Moreover, these cusps are at *equal distances*. Similar singularities of the DOS for NS systems have already been found by de Gennes et al.<sup>7</sup> as well as in the numerical works of Richter et al.<sup>15</sup> (for NS systems), Nazarov et al.<sup>13</sup> (for Andreev billiard), and Šipr et al.<sup>20</sup> (for SNS systems). In this section we investigate the singularities in the DOS for the NS systems shown in Fig. 1.

Several authors<sup>9,13–15</sup> have already derived the Bohr-Sommerfeld approximation to the density of states,

$$\rho_{BS}(\varepsilon) = M \int_0^\infty ds P(s) \sum_{n=0}^\infty \delta\left(\varepsilon - \left(n + \frac{1}{2}\right) \frac{\pi \hbar v_F}{s}\right), \quad (41)$$

where  $M$  is the number of modes in the superconducting leads connected to the normal billiard, and  $P(s)$  is the classical probability that an electron entering the billiard exits after a path length  $s$ . Starting from our quantization rule given in Eq. (26) we re-derive Eq. (41) in this section, and give an explicit expression of the probability  $P(s)$  in terms of  $\Phi_m(\varepsilon)$ . We shall show that  $P(s)$  is singular at some  $s$  resulting in the singularities of the DOS. These singularities correspond to the cusps in the integrated DOS  $N(\varepsilon)$ . It turns out that the simple Bohr-Sommerfeld approximation to the DOS is a good approach to understand the singularities in the DOS provided that  $P(s)$  is approximated correctly for small  $s$ .

The solution of Eq. (26) gives the discrete energy levels for the NS systems. Since  $\varepsilon \ll E_F$ , one can Taylor expand the LHS of Eq. (26) in terms of  $\varepsilon$  and find

$$\varepsilon_{n,m} = \frac{\left(n + \frac{1}{2}\right) \pi}{\Phi'_m(0)}, \quad (42)$$

where  $\Phi'_m(0)$  denotes the derivative of  $\Phi_m(\varepsilon)$  with respect to  $\varepsilon$ , evaluated at the Fermi energy, i.e.  $\varepsilon = 0$ . For the NS box systems  $m = 1, 2, \dots, M$ , where the energy dependent  $M$  is the number of ‘transverse modes’. For the NS disk systems  $|m| < M$ , where  $M$  is the maximum of the angular momentum quantum number  $m$  for the Andreev states. We consider only the positive energy spectrum, therefore  $n \geq 0$ . Here we take the box geometry. The following expressions for disk geometry can be obtained straightforwardly by taking into account the fact that the set of  $m$  is different in this case. Thus  $M$  has a different meaning for box and disk geometries. We shall always indicate how to convert the box geometry results to the disk geometry case. To get Eq. (42), the phase term in Eq. (26) due to Andreev reflection,  $\arccos(\varepsilon/\Delta_0)$  was approximated by  $\pi/2$ , which is valid for  $\varepsilon \rightarrow 0$ . Later a better approximation will be given by Taylor expanding the phase term, too. The density of states is then

$$\rho(\varepsilon) = \sum_{n=0}^{\infty} \sum_{m=1}^M \delta(\varepsilon - \varepsilon_{n,m}) = \sum_{n=0}^{\infty} \sum_{m=1}^M \int ds \delta\left(\varepsilon - \frac{(n + \frac{1}{2}) \hbar \pi v_F}{s}\right) \delta(s - \hbar v_F \Phi'_m(0)). \quad (43)$$

We have seen in Secs. III A and III B that  $\hbar \Phi_m(0)$  is the classical action for the electron with Fermi energy moving in the N region between two subsequent bounces at the superconductor. Thus,  $s = \hbar v_F \Phi'_m(0)$  is the path length of the trajectories of the electron between two successive bounces at the NS interface. We now show that the above expression for  $\rho(\varepsilon)$  can be rewritten in the same form as in (41), which makes it possible to express the probability  $P(s)$  in terms of  $\Phi_m(\varepsilon)$ .

Applying the Poisson formula<sup>31,22</sup> for the summation over  $m$  in (43) we have

$$\rho(\varepsilon) = \sum_{n=0}^{\infty} \int_0^{\infty} ds \delta\left(\varepsilon - \frac{(n + \frac{1}{2}) \hbar \pi v_F}{s}\right) \sum_{k=-\infty}^{\infty} \int_{1/2}^{M+1/2} dm \delta(s - \hbar v_F \Phi'_m(0)) e^{i2\pi km}. \quad (44)$$

Keeping only the non-oscillating term ( $k = 0$ ) in the sum over  $k$ , and then performing the integral over  $m$  we obtain the same Bohr-Sommerfeld approximation to the DOS as in Eq. (41). The probability  $P(s)$  is given by

$$P(s) = \frac{\Theta(M - m^*) \Theta(m^* - 1)}{M \hbar v_F \left| \frac{\partial \Phi'_m(0)}{\partial m} \right|_{m=m^*}}, \quad (45)$$

where the  $s$ -dependent  $m^*$  satisfies

$$\hbar v_F \Phi'_m(0) \Big|_{m=m^*} = s. \quad (46)$$

$\Theta(x)$  is the Heaviside function. Note that the probability  $P(s)$  is normalized to 1, i.e.  $\int_0^{\infty} P(s) ds = 1$ . For disk geometry the numerator in (45) has to be replaced by  $\Theta(M - |m^*|)/2$ , and the necessary replacement in (41) is  $M \rightarrow 2M$ . Our main result is that the probability  $P(s)$  is expressed in terms of  $\Phi_m(\varepsilon)$ , which has already been determined for box and disk geometries of the NS system (see Eqs. (30) and (A9)).

Performing the integral over  $s$  in Eq. (41) one finds

$$\rho_{BS}(\varepsilon) = \frac{M}{\varepsilon} \sum_{n=0}^{\infty} s_n(\varepsilon) P(s_n(\varepsilon)), \quad (47)$$

where

$$s_n(\varepsilon) = \frac{(n + \frac{1}{2}) \pi \hbar v_F}{\varepsilon} = \frac{(n + \frac{1}{2}) 2\pi}{k_F} \frac{E_F}{\varepsilon}. \quad (48)$$

Similarly, the counting function  $N_{BS}(\varepsilon) = \int_0^{\varepsilon} d\varepsilon' \rho_{BS}(\varepsilon')$  can be easily found

$$N_{BS}(\varepsilon) = M \sum_{n=0}^{\infty} \int_{s_n(\varepsilon)}^{\infty} P(s) ds. \quad (49)$$

Both in (47) and (49) we have to replace  $M$  by  $2M$  in the case of NS disk systems as  $M$  has a different meaning in this case. The above results are valid only for small  $\varepsilon$ . Numerical results show that a better approximation of the counting function can be obtained by Taylor expanding the phase shift related to the Andreev reflection:  $\arccos(\varepsilon/\Delta_0) \approx \pi/2 - \varepsilon/\Delta_0$ . Then the discrete energy levels are given by

$$\varepsilon_{n,m} = \frac{(n + \frac{1}{2}) \pi}{\Phi'_m(0) + \frac{1}{\Delta_0}}. \quad (50)$$

Carrying out the same procedures as before one finds that the counting function  $N_{BS}(\varepsilon)$  is still given by Eq. (49) after the replacement

$$s_n(\varepsilon) \rightarrow s_n(\varepsilon) - \xi_0 \quad (51)$$

is made in (48). Here  $\xi_0 = \xi(\varepsilon = 0) = \hbar v_F/\Delta_0 = 2E_F/(k_F \Delta_0)$  is the coherence length at the Fermi energy (see Eq. (A8)).

In the following two subsections we shall calculate  $P(s)$  and the counting function  $N_{\text{BS}}(\varepsilon)$  for NS box and disk systems. We shall see that the probability  $P(s)$ , more precisely  $sP(s)$ , is singular at some  $s_{\text{sing}}$  for both NS systems. Then, if  $s_{\text{sing}}$  is known, one can determine from (51) the energies where  $P(s_n(\varepsilon))$ —and consequently (see Eq. (47)) the density of states  $\rho_{\text{BS}}(\varepsilon)$ —is singular:

$$\varepsilon_n^{(\text{sing})} = \frac{(n + 1/2)\pi}{1 + s_{\text{sing}}/\xi_0} \Delta_0, \quad (52)$$

which is valid for all  $n$  for which  $\varepsilon_n^{(\text{sing})} < \Delta_0$ . Note that this expression can be applied to those normal systems attached to a superconductor for which  $sP(s)$  is singular. It is clear from this expression that these singularities are at *equal* distances. The analytical behavior of  $P(s)$ , and thus, the existence of the singularities in the DOS for perfect NS interface inherently depends on the geometry of the isolated normal billiard. Once  $sP(s)$  is a singular function of  $s$  (because of the shape of the normal region), then the subsequent singularities in the DOS are at equal distances. We shall see that from the exact calculation of the energy eigenvalues for NS box and disk systems the positions of the singularities in the DOS agree very well with those given by the above derived approximate expression. We would like to emphasize that the second term in the denominator of Eq. (52) resulted from the Taylor expansion of  $\arccos(\varepsilon/\Delta_0)$  which is the phase shift due to the Andreev reflection. We shall see below that this extra term involving the coherence length  $\xi_0$  in Eq. (52) is necessary for getting good agreements between the exact and that of predicted by Eq. (52) for the position of the singularities.

### A. Singularities in DOS for Box

In Sec. III A we have calculated  $\Phi_m(\varepsilon)$  for the NS box system with perfect interface. Inserting  $\Phi_m(\varepsilon)$  given by (30) into Eqs. (45) and (46) one finds

$$P(s) = \frac{4d^2}{s^3 \sqrt{1 - \left(\frac{2d}{s}\right)^2}} \Theta(s - s_{\text{min}}), \quad (53)$$

where  $s_{\text{min}} = 2d/\sqrt{1 - 1/M^2}$  and  $M = k_F W/\pi$  is the number of ‘transverse modes’. For a large number of transverse modes, i.e.  $M \gg 1$  we have  $s_{\text{min}} = 2d$ . Notice that the same result can be found for  $P(s)$  by simple geometrical considerations<sup>32</sup>.  $P(s)$  is singular at  $s_{\text{sing}} = 2d$ , therefore the DOS is singular at the energies given by (52). The DOS can be calculated from Eq. (47) in Bohr-Sommerfeld approximation. In Fig. 7 the normalized DOS,  $\rho_{\text{BS}}(\varepsilon)/(2\rho^{(\text{N})})$  is plotted in Bohr-Sommerfeld approximation together with its slope for  $\varepsilon \rightarrow 0$ . Here  $\rho^{(\text{N})} = 2m/\hbar^2 (A/4\pi)$  is the DOS of the normal box of area  $A = dW$ .

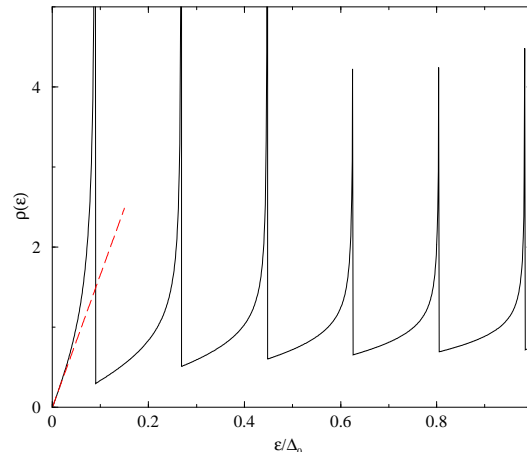


FIG. 7. The Bohr-Sommerfeld approximation of the DOS for the box geometry—normalized by the DOS of a normal billiard of area  $A = dW$  (solid line)—and its slope for  $\varepsilon \rightarrow 0$  (dashed line) as functions of  $\varepsilon/\Delta_0$ . The parameters are the same as in Fig. 2. With these parameters  $2d/\xi_0 = 16.57$ .

From (48) it is clear that the DOS for small  $\varepsilon$  is dominated by the large  $s$  behavior of  $P(s)$ . According to (53),  $P(s) \rightarrow 4d^2 s^{-3}$  in this case. Thus,

$$\frac{\rho_{\text{BS}}(\varepsilon)}{2\rho^{(\text{N})}} \rightarrow \frac{\varepsilon}{\pi E_T}, \quad \text{for } \varepsilon \rightarrow 0, \quad (54)$$

where  $\rho^{(\text{N})} = (2m_{\text{N}}/\hbar^2) A/(4\pi)$  is the DOS for the isolated billiard of area  $A = dW$  and  $E_T = M/(4\pi\rho^{(\text{N})})$  is the Thouless energy defined in Refs. 9,15. This result is shown by the dashed line in Fig. 7. For small energies  $\varepsilon$  the DOS is proportional to  $\varepsilon$  in agreement with the findings of Melsen et al.<sup>9,10</sup> and Ihra et al.<sup>15</sup>. However, the slope of  $\rho_{\text{BS}}(\varepsilon)/2\rho^{(\text{N})}$  is less than what these authors found. The reason is that the geometries of the billiards they studied are slightly different from our box geometry. Namely, the width  $w$  of their superconducting lead is smaller than the side length of the billiard with which it is in contact. In these geometries, by quantum mechanical calculations, Ihra et al.<sup>15</sup> found 3 pronounced peaks in the DOS approximately at  $\varepsilon/E_T = 3.1, 8.3, 13.4$  (see Fig. 3. in that paper). They mention that similar peaks were observed for other parameter values of the billiards. If we assume that these peaks are indeed singularities in the DOS then fitting these data to Eq. (52) one finds that  $P(s)$  is singular at  $s = s_{\text{sing}} \approx 1.1L_T$ , where  $L_T = \pi a^2/w$  is the Thouless length used in their paper. The Thouless length is related to the mean escape time by  $\tau_{\text{esc}} = L_T/v_F$  for the billiard which is open along the superconducting lead. Since it is reasonable to expect  $P(s)$  to be high around  $s = L_T$ , our theory about the singularities in the DOS may explain the reason for the pronounced peaks in the DOS observed by Ihra and his coworkers<sup>15</sup>. They have calculated  $P(s)$  for another set of parameters of the billiard, and a peak can also be seen around  $s = L_T$  in Fig. 2. in their work. However, to confirm the existence of the singularity in  $P(s)$  one needs to calculate  $P(s)$  on a finer scale than in Fig. 2. of their paper.

To avoid the errors of numerical differentiation, we shall compare the counting function obtained from the quantum mechanical calculations (see Eq. (19)) with the counting function  $N_{\text{BS}}(\varepsilon)$  in Bohr-Sommerfeld approximation. Using (49) and (53), and performing the integration, we obtain

$$N_{\text{BS}}(\varepsilon) = M \sum_{n=0}^{\infty} f(s_n(\varepsilon)), \quad (55)$$

where

$$f(s) = \begin{cases} 1, & \text{if } s \leq 2d, \\ 1 - \sqrt{1 - 4d^2/s^2}, & \text{if } s > 2d, \end{cases} \quad (56)$$

and  $s_n(\varepsilon)$  is given in Eq. (51). The above derived counting function  $N_{\text{BS}}(\varepsilon)$  is plotted in Fig. 8 together with the exact counting function.

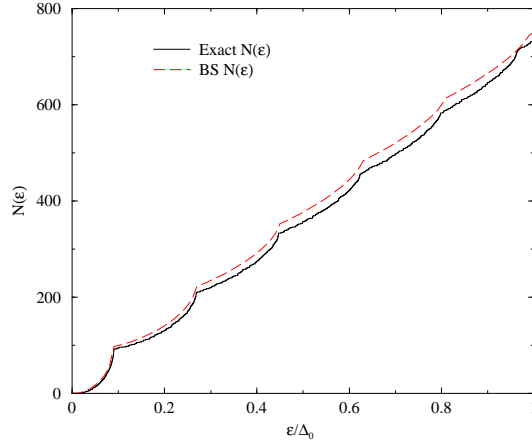


FIG. 8. The exact counting function  $N(\varepsilon)$  (solid line) and  $N_{\text{BS}}(\varepsilon)$  given in (55) (dashed line) as functions of  $\varepsilon/\Delta_0$  for the box geometry. The parameters are the same as in Fig. 2.

One can see that the agreement is excellent at low energies (below the second cusp) but for higher energies the exact counting function is smaller than the approximated one. However, the positions of the singularities agree quite well in the two curves. Slight deviations are observed only for the last two cusps. The same was found for other parameter ranges. Thus, our expression (52) for the positions of the singularities in the DOS results in an excellent agreement with exact quantum mechanical calculations. Our result may highlight the origin of the singularities of the DOS. One can see that  $P(s)$  is singular at  $s = 2d$ , which corresponds to the classical orbits when the electron enters the box parallel to the  $x$  axis and is reflected back at the wall. The enhanced return probabilities for these orbits are

quite obvious. These are the orbits which result in the singularities of the DOS. It is also clear from this expression that the singularities are at equal distances.

The expression for the positions of the singularities given by Eq. (52) can be applied to other NS systems, e.g. that studied by de Gennes and Saint-James<sup>7</sup>. They considered an NS system in which a normal film of width  $a$  is in contact with a semi-infinite superconductor. This geometry of the NS system is similar to our NS box system shown in Fig. 1a. The authors also found singularities in the DOS for parameter values  $2a/\xi_0 = 2.5, 8, 20$ . Using Fig. 1 of their paper we measured the positions of the singularities in the DOS, labeled them as  $n = 0, 1, 2, \dots$ , and plotted them in Fig. 9 (circles and squares) against  $n$ . For  $2a/\xi_0 = 2.5$  they found only one singularity which is not shown in Fig. 9. We can expect that the probability  $P(s)$  for this system, similarly to our box geometry, is singular at  $s = 2a$ . Thus, assuming that  $s_{\text{sing}} = 2a$  we calculated the positions of the singularities from Eq. (52) and also plotted them in Fig. 9. For clarity, these points are connected by lines.

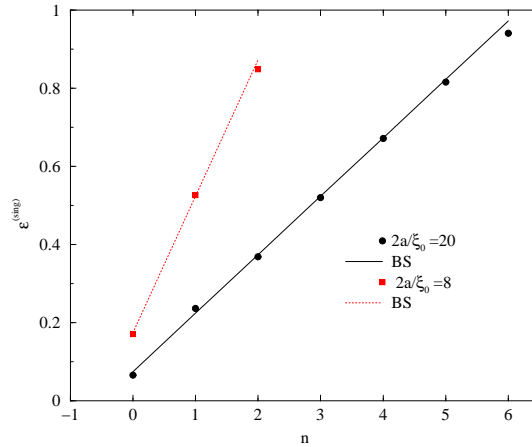


FIG. 9. The positions (in units of  $\Delta_0$ ) of the singularities of the DOS obtained from Fig. 1 in the work of de Gennes and Saint-James<sup>7</sup> (circles and squares) and from our expression (52) (for clarity, the points are connected by lines).

It can be seen from the figure that the agreement is excellent. Even for  $2a/\xi_0 = 2.5$  (when there is only one singularity) the position of the singularity agrees very well with that found from our expression (52). We note that to achieve such a good agreement the Taylor expansion of the phase shift  $\arccos(\varepsilon/\Delta_0)$  in terms of  $\varepsilon$  was necessary. Therefore, to understand the nature of the singularities one needs to take into account not only the singular behavior of  $P(s)$  which depends on the geometry of the billiard but a more physically related quantity, namely the coherence length of the superconductor.

Finally, we mention that Lodder and Nazarov<sup>13</sup> also found singularities in the DOS for different shapes of Andreev billiards. Our results suggest that these singularities are related to some special classical orbits which are characteristic of the specific geometry. Sipr et al.<sup>20</sup> studied SNS systems taking fully into account the motion parallel to the infinite interface. Their results also show singularities in the DOS. We believe that these singularities are also related to some special classical orbits which give rise to a singular behavior of the probability  $P(s)$ , similarly to the NS systems studied in this paper.

We also calculated the energy levels in the case of non-perfect NS interface. Solving the secular equation (19) numerically, the obtained counting function  $N(\varepsilon)$  is shown in Fig. 10. We have used the same parameters for describing the mismatch in the Fermi energies and the effective masses as in Ref. 33, namely  $r_k = k_F^{(N)}/k_F^{(S)}$ ,  $r_v = v_F^{(N)}/v_F^{(S)}$ . The strength of the tunnel barrier is given by  $Z$ .

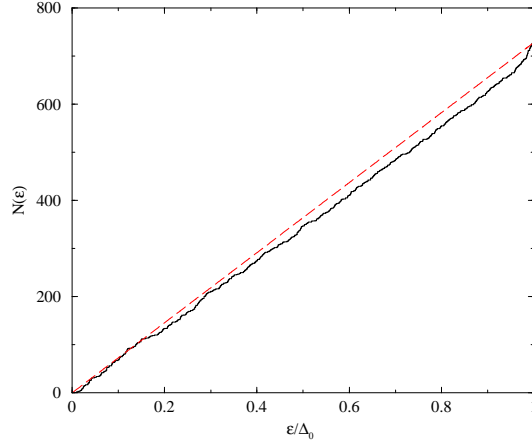


FIG. 10. The counting function  $N(\varepsilon)$  as a function of  $\varepsilon/\Delta_0$  (solid line) for the box geometry when the interface is not perfect. The parameters are:  $d/W = 3$ ,  $k_F^{(N)}W/\pi = 87.9$ ,  $\Delta_0/E_F^{(N)} = 0.02$ ,  $r_k = 0.007$ ,  $r_v = 0.1$  and with no tunnel barrier, i.e.  $Z = 0$ . The Weyl formula in leading order (see text) is given by the dashed line.

It can be seen from the figure that for a non-perfect NS interface the cusps in the counting function are 'washed out'. It is related to the fact that the normal reflections at the interface are enhanced. The same is true for  $Z \neq 0$ . In Sec. III A we have found that in leading order the Weyl formula is given by  $\tilde{N}(\varepsilon) \approx 2\varepsilon\rho^{(N)}$ , where  $\rho^{(N)} = 2m/\hbar^2 (A/4\pi)$  is the density of states for the isolated N region of area  $A = Wd$ . This is shown by the dashed line in Fig. 10. One can see from the figure that the exact counting function can be approximated by the above Weyl formula. This implies that for non-perfect NS interfaces the effect due to the Andreev reflection is less significant, and the system behaves as a normal metal regarding the energy levels.

### B. Singularities in DOS for disk

The maximum angular momentum quantum number,  $M_{AS}$  for Andreev states has been determined in Sec. III B after Eq. (34). To have a better physical picture of these states we now give an estimation for  $M_{AS}$  based on semiclassical considerations. It is easy to see that the angular momentum (in units of  $\hbar$ ) of the rays shown in Fig. 5a is  $m = k_F R_N \sin(\alpha/2)$ , where  $\alpha$  is the angle between the two rays at the outer circle. Rays that are tangent to the inner circle have maximal angular momentum, in which case  $\sin(\alpha/2) = R_S/R_N$ . These are the trajectories which still reach the superconductor so that they belong to the Andreev states. Thus, the maximal angular momentum  $m$  for the Andreev states is  $k_F R_S$ . This is a good estimate for  $M_{AS}$  given after Eq. (34).

In subsection III B we have seen that for  $R_S \gg \xi(\varepsilon)$  and for perfect NS interface the energy levels for NS disk systems can be classified into Andreev and whispering gallery states to a good approximation. We first consider the Andreev states. Inserting  $\Phi_m(\varepsilon)$  given by Eq. (A9) into Eqs. (45) and (46), one finds after some algebra

$$P(s) = \frac{1}{4s^2 R_S} \frac{s_{\max}^4 - s^4}{\sqrt{[s_{\max}^4/s_{\min}^2 - s^2][s^2 - s_{\min}^2]}} \Theta(s_{\max} - s) \Theta(s - s_{\min}), \quad (57)$$

where  $s_{\min} = 2(R_N - R_S)$  and  $s_{\max} = 2\sqrt{R_N^2 - R_S^2}$ . The two Heaviside functions come from the factor  $\Theta(M - |m^*|)/2$  (see the text after Eq. (46)) when we change to the variable  $s$ . Here  $s_{\min}$  and  $s_{\max}$  correspond semiclassically to the smallest and the largest path lengths of the orbits related to the Andreev states. Obviously,  $s_{\min}$  equals to the path length of those orbits for which the trajectory of the electrons between two successive bounces at the NS interface is along the radius of the two concentric circles. The trajectories of the electrons corresponding to the maximal path length for Andreev states are those which are tangent to the inner circle of radius  $R_S$ . The probability  $P(s)$  is zero for  $s_{\min} > s > s_{\max}$  and normalized to one. Note that in deriving (57), the solution of Eq. (46) is twofold for  $m^*$  resulting in an extra factor 2 in  $P(s)$ . Notice that the same result can be found for  $P(s)$  by simple geometrical considerations<sup>32</sup>. One can see that  $P(s)$  is singular at  $s = s_{\min}$ . The contributions of the Andreev states to the DOS in Bohr-Sommerfeld approximation is given by Eq. (47), which reads

$$\rho_{AD}(\varepsilon) = \frac{2k_F R_S}{\varepsilon} \sum_{n=0}^{\infty} s_n(\varepsilon) P(s_n(\varepsilon)), \quad (58)$$



where  $P(s)$  is given by (57) and  $s_n(\varepsilon)$  by (51). Since there is a maximum path length  $s$  for Andreev states, the sum over  $n$  in (47) is indeed finite.

Next, we consider the contribution of the whispering gallery states to the DOS. After differentiations with respect to  $\varepsilon$  in Eq. (37) and replacing the summations over  $m$  by integrals the calculations can be carried out analytically (here we used  $M_{\text{wgs}} \approx k_e R_S$  and neglected the higher order terms in  $\varepsilon/E_F$ ). It is found that the DOS is *constant* in  $\varepsilon$  and is given by

$$\rho_{\text{wgs}} = \frac{(k_F R_N)^2}{2E_F} \left[ 1 - \frac{2}{\pi} \left( \frac{R_S}{R_N} \sqrt{1 - \left( \frac{R_S}{R_N} \right)^2} + \arcsin \frac{R_S}{R_N} \right) \right]. \quad (59)$$

Thus, the total DOS for the NS disk system in Bohr-Sommerfeld approximation is  $\rho_{\text{wgs}} + \rho_{\text{AD}}(\varepsilon)$ . Since  $P(s)$  is a singular function, the DOS becomes singular at the energies given by (52) with  $s_{\text{sing}} = 2(R_N - R_S)$ . In Fig. 11 we plotted the normalized DOS,  $\rho_{\text{BS}}(\varepsilon)/(2\rho^{(\text{N})})$  in Bohr-Sommerfeld approximation, where  $\rho^{(\text{N})} = 2m/\hbar^2(A/4\pi)$  is the DOS of the normal circular annular billiard of area  $A = (R_N^2 - R_S^2)\pi$ .

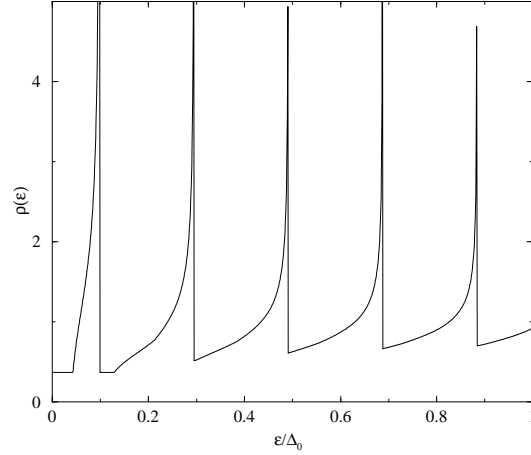


FIG. 11. The normalized DOS (see text) in Bohr-Sommerfeld approximation as a function of  $\varepsilon/\Delta_0$  for the disk geometry. The parameters are the same as in Fig. 4. With these parameters  $s_{\text{min}}/\xi_0 = 15.0$ .

One can see that the DOS does not tend to zero as  $\varepsilon \rightarrow 0$ , contrary to the box geometry case. The non-vanishing DOS is due to the constant contribution of the whispering gallery states given by Eq. (59).

Again, one can determine the counting function  $N_{\text{BS}}(\varepsilon)$  by integrating the DOS. Using Eqs. (49) and (57) the integral can be performed analytically, and

$$N_{\text{BS}}(\varepsilon) = \rho_{\text{wgs}} \varepsilon + 2k_F R_S \sum_{n=0}^{\infty} f(s_n(\varepsilon)) \Theta(s_{\text{max}} - s_n(\varepsilon)) \quad (60)$$

is obtained, where

$$f(s) = \begin{cases} 1, & \text{if } s \leq s_{\text{min}}, \\ 1 - \frac{\sqrt{[s_{\text{max}}^4/s_{\text{min}}^2 - s^2][s^2 - s_{\text{min}}^2]}}{4sR_S}, & \text{if } s_{\text{min}} < s \leq s_{\text{max}}, \end{cases} \quad (61)$$

and  $s_n(\varepsilon)$  is given by (51). Note that the infinite sum over  $n$  in (60) is indeed a finite one due to the Heaviside function. Using Eqs. (19)-(20) we calculated the exact energy levels for the NS disk system. In Fig. 12 the exact counting function  $N(\varepsilon)$  and  $N_{\text{BS}}(\varepsilon)$  are plotted for perfect interface (no mismatch and zero tunnel barrier).

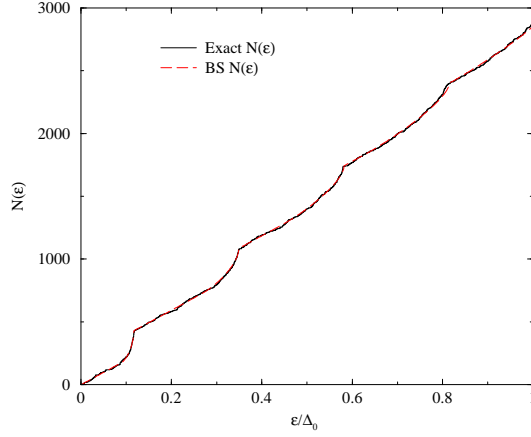


FIG. 12. The exact counting function  $N(\varepsilon)$  (solid line) and  $N_{BS}(\varepsilon)$  given in (60) (dashed line) as functions of  $\varepsilon/\Delta_0$  for the disk geometry. The parameters are the same as in Fig. 6. Then  $s_{\min}/\xi_0 = 12.5$ .

One can see that the agreement between the exact counting function and that obtained from the Bohr-Sommerfeld approximation is excellent for all energies below the gap. To see the agreement, the details of Fig. 12 – up to the first two cusps – are enlarged in Fig. 13.

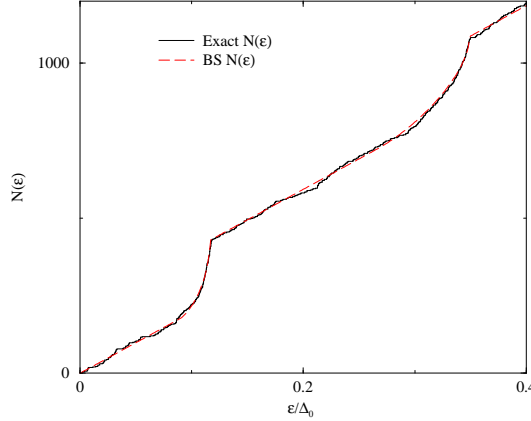


FIG. 13. Enlarged portion of Fig. 12.

Similarly, very good agreements were found for other parameter ranges of the NS disk systems with perfect interface.

In Fig. 4 one can see that the energy levels (for each radial quantum number  $n$ ) as functions of  $m$  are approximately constant as  $m \rightarrow 0$ . Thus, the DOS should diverge because it is proportional to the reciprocal of the derivative of  $\varepsilon_{mn}$  with respect to  $m$  (assuming that  $m$  is a continuous variable). The positions of the singularities of the DOS coincide with the energies  $\varepsilon_{mn}$  at  $m = 0$  for all possible  $n$ . The angular momentum quantum number  $m = 0$  semiclassically corresponds to the radial orbits of the electron between the inner and outer circles. Applying the Bohr-Sommerfeld quantization rule for the electrons and the Andreev reflected holes along the radius one finds

$$[k_e(\varepsilon) - k_h(\varepsilon)](R_N - R_S) = n\pi + \arccos(\varepsilon/\Delta_0). \quad (62)$$

Note that this equation can also be derived from the quantization condition given in Eq. (26). The solutions of Eq. (62) agree very well with the energies in Fig. 4 at  $m = 0$ . Therefore, the singularities of the DOS are related to the classical orbits along the radial directions.

We also calculated the energy levels in the case of non-perfect NS interface. Solving the secular equation (19) numerically, the counting function  $N(\varepsilon)$  is shown in Fig. 14.

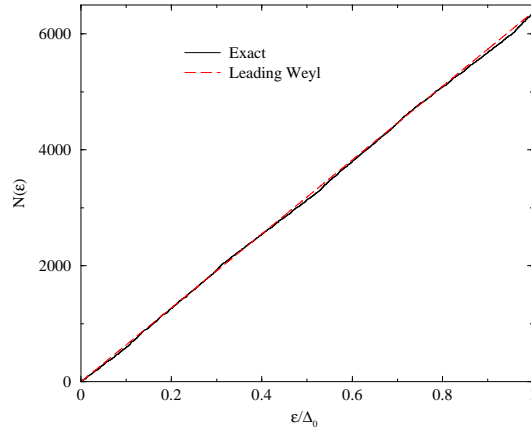


FIG. 14. The exact counting function  $N(\varepsilon)$  (solid line) and the leading term of the Weyl formula  $\tilde{N}(\varepsilon)$  (dashed line) as functions of  $\varepsilon/\Delta_0$  for the NS disk geometry when the interface is not perfect. The parameters are  $R_S/R_N = 7/10$ ,  $k_F^{(N)} R_S = 350$ ,  $\Delta_0/E_F^{(N)} = 0.1$ ,  $r_k = 0.01$ ,  $r_v = 0.1$ , and tunnel barrier,  $Z = 0$ .

It can be seen from the figure that for non-perfect NS interface the cusps in the counting function are 'washed out' similarly to the case of NS box systems. This is related to the fact that the normal reflections at the interface are enhanced. Our numerical results show that the cusps also disappear for  $Z \neq 0$ . Using the Weyl formula derived in Sec. III B we found that  $\tilde{N}(\varepsilon) = 2\rho^{(N)}\varepsilon$  in leading order, where  $\rho^{(N)} = (2m/\hbar^2) (R_N^2 - R_S^2)/4$  is the density of states for normal annular billiard with inner radius  $R_S$  and outer radius  $R_N$ . In Fig. 14 this is drawn by a dashed line. One can see that this Weyl formula is a good approximation for the exact counting function in the case of non-perfect interfaces. The result shows that the role of normal reflections dominates over Andreev reflections, and thus the Weyl formula agrees approximately with that for the circular annular billiard without superconducting region.

## V. 'PHASE DIAGRAM' FOR NS DISK SYSTEMS

In our studies of the energy levels of the NS disk systems we have assumed so far that the energy dependent coherence length  $\xi(\varepsilon) = \hbar v_F / \sqrt{\Delta_0^2 - \varepsilon^2}$  is much smaller than  $R_S$  (see the text after Eq. (A8)). In this section we shall discuss the case when  $\xi(\varepsilon) \gg R_S$ , i.e. when  $\varepsilon \rightarrow \Delta_0$ . The imaginary part of  $q_e R_S \approx k_F R_S + i R_S / \xi(\varepsilon)$  is then negligible, and  $k_e R_S \approx q_e R_S$ . Thus, in the determinant  $D_m^{(e)}(\varepsilon)$  given in Eq. (23) the arguments of the Bessel functions are almost equal. We now consider the perfect NS interface ( $Z = 0$  and  $m_N = m_S$ ). Subtracting the second column from the first one in the determinant, the ratio  $J_m(k_e R_N) / Y_m(k_e R_N)$  can be factored out. It turns out that the remaining determinant is non-zero for  $\varepsilon < \Delta_0$ . Thus, similarly to the whispering gallery states discussed in Sec. III B, it holds to a very good approximation that  $D_m^{(e)}(\varepsilon)$  (as a function of  $\varepsilon$ ) has zeros whenever  $J_m(k_e R_N) = 0$  for *all*  $m$ . This corresponds to the energy levels of a circular billiard of radius  $R_N$  for electron-like quasiparticles. The same is true for the hole-like quasiparticles, i.e. their energy levels are the solutions of  $J_m(k_h R_N) = 0$  for all  $m$ . In summary, we found that for  $\xi(\varepsilon)/R_S \gg 1$  the NS disk system behaves as a normal full disk, while in the opposite case the energy levels of the system have a 'mixed phase' character, in which Andreev states and whispering gallery states coexist (see Sec. III B). We shall call the first case a 'full disk phase' (FD). According to our numerical results, it is safe to say that the MP and FD can be distinguished very well by the ratio  $\xi(\varepsilon)/R_S$ . We found mixed phase for  $\xi(\varepsilon)/R_S < 2$  and FD phase for  $\xi(\varepsilon)/R_S > 2$ .

As it is known, the Andreev approximation is valid only for  $\Delta_0/E_F \ll 1$ . If we assume some critical value, say  $\Delta_0/E_F = 0.1$ , then for  $k_F \xi_0 = 2E_F/\Delta_0 < 20$  the Andreev approximation is not valid and normal reflection at the NS interface dominates over Andreev reflection. The system looks like an annular billiard (without superconductor region). We shall call this case an 'annular phase' (AP). As we have seen in the Fig. 14, the non-perfect interface also results in an enhanced normal reflection and the character of the energy levels again corresponds to a circular annular billiard (annular phase).

We calculated the exact energy levels for different parameters and compared with those obtained for the full disk and for circular annular disk. In this way, we can classify the NS disk systems into the MP, FD and AP phase regions. The crossovers between the three 'phases' are not sharp and depend on the energy, too. It turns out that the three phases can be characterized by two parameters,  $k_F R_S, k_F \xi(\varepsilon)$ . These are the relevant parameters for the NS disk systems and each pair corresponds to one of the phases. Thus, a so-called phase diagram can be given for the different

phases. The boundaries of these phases are not so sharp, however. Far from the boundaries the given phase becomes dominating. In Fig. 15 the three different phases are shown.

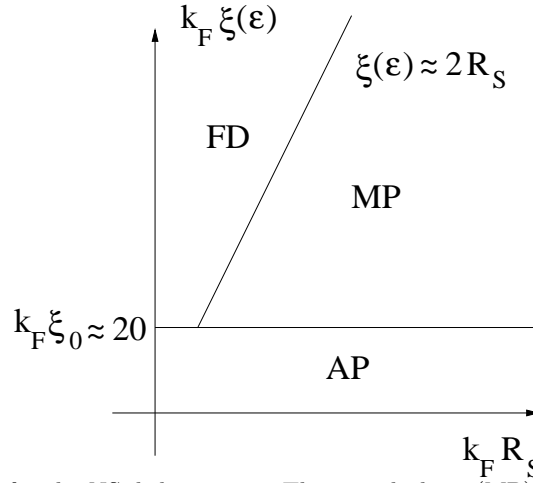


FIG. 15. Schematic phase diagram for the NS disk systems. The mixed phase (MP) is bounded by the lines  $k_F \xi_0 \approx 20$  and  $\xi(\varepsilon) \approx 2R_S$ . The full disk phase (FD) is bounded by the line  $k_F R_S = 0$ , the line  $k_F \xi_0 \approx 20$  and the line  $\xi(\varepsilon) \approx 2R_S$ . The annular phase (AP) is below the line  $k_F \xi_0 \approx 20$ .

## VI. CONCLUSIONS

We investigated the energy spectrum of NS box and disk systems using the BdG equation. Matching the wave functions at the NS interface we derived a secular equation whose solutions give the energy spectrum of the system. The mismatch in the Fermi wave numbers and the effective masses of the normal system and the superconductor, as well as the tunnel barrier is included in the calculation. Rewriting the secular equation a simple quantization condition was derived. Equation (26) is a central result and serves as a starting point for further theoretical studies in this paper. Using this quantization condition (a) we derived for both NS systems with perfect interfaces a Weyl formula for the counting function, (b) by re-deriving the commonly used Bohr-Sommerfeld approximation to the DOS we presented an explicit expression for the probability  $P(s)$  in terms of the classical action of the electron moving in the N region between two successive bounces at the NS interface. The numerically exact calculations are in very good agreement with our Weyl formula and the Bohr-Sommerfeld approximation. The singularities in the DOS obtained from our exact calculations can be successfully explained by using the correct probability function  $P(s)$ .  $P(s)$  is a singular function of  $s$  both for NS box and disk systems. According to our theory concerning the singularities, this implies that the singularities of the DOS are located at equal distances from each other. A simple formula is given for the location of the singularities. We demonstrated that it can be applied for the system studied by de Gennes et al.<sup>7</sup>, and it may as well give the reason for the significant peaks observed by Ihra et al.<sup>15</sup> in their numerical calculations. We show that the singularities in  $P(s)$  are related to some special classical trajectories of the electron moving in the N region hitting the NS interface.

In the case of NS disk systems the DOS is constant as the energy gets close to the Fermi level. This is, at first sight, in contrast to the common belief that for integrable billiards the DOS should go to zero as the energy tends the Fermi level. We pointed out that in this NS disk system the whispering gallery states give the non-vanishing DOS at the Fermi level. However, the Andreev states still have no contribution to the DOS. In the disk system the Andreev and the whispering gallery states coexist (so-called mixed phase). Depending on the geometry of the disk and the material parameters, we sketch a kind of phase diagram to classify the energy spectra into three classes: (i) mixed phase, (ii) full disk, (iii) annular disk. If the coherence length is much larger than the diameter of the superconducting region, the spectrum corresponds to the full disk phase. The electrons travel thorough the S region without Andreev reflection. When the Andreev approximation fails, the normal reflection is enhanced at the NS interface and the system behaves as an annular circular billiard. This is also the case when there is a tunnel barrier at the NS interface or a mismatch between the effective masses and the Fermi wave numbers of the normal and superconducting regions.

An interesting extension of the study presented in this paper may be the investigation of the role that the geometry of the normal billiard plays in the singularities of the DOS. Under what conditions do such singularities exist? Does the energy spectrum at higher energies show some special structure in chaotic billiards? How can the Weyl formula (derived for NS box and disk systems) be extended for other integrable and chaotic billiards? Our quantization

method can also be applied for NS disk in the presence of a magnetic field. In this case, besides Andreev states and whispering gallery states (more specifically edge states) one has to take into account the Landau levels that appear in the spectrum in the presence of strong magnetic fields. These give rise to a much more complex energy spectrum than a zero magnetic field. Another relevant question is the study of the counting function in these systems. Further work along these lines is in progress.

## ACKNOWLEDGMENTS

One of us (J. Cs.) would like to thank C. W. J. Beenakker, U. Zülicke, T. Geszti, Z. Kaufmann and A. Piróth for useful discussions. This work supported in part by the European Community's Human Potential Programme under contract HPRN-CT-2000-00144, Nanoscale Dynamics, and the Hungarian Science Foundation (OTKA TO25866 and TO34832).

## APPENDIX A: CALCULATION OF THE PHASE $\Phi_m(\varepsilon)$

It is clear for symmetry reasons that the eigenstates with quantum numbers  $m$  and  $-m$  are degenerate (except for  $m = 0$ ), thus it is enough to consider the states  $m \geq 0$ . In the Andreev approximation ( $\Delta_0/E_F \ll 1$ ) we take  $k_m^{(e)} \approx q_m^{(e)}$  in places where they are multiplied by the Bessel functions in  $D_m^{(e)}(\varepsilon)$  but in the arguments of the Bessel functions we keep them to be different. As we shall see, different methods are necessary to approximate the determinant  $D_m^{(e)}(\varepsilon)$  for different ranges of  $m$ . The Debye asymptotic expansion<sup>34</sup> will be used to approximate the determinant for  $|m| < k_e R_S - \sqrt[3]{k_e R_S}$ . In this expansion the Bessel functions with the real argument  $x$  for  $0 < m < x - \sqrt[3]{x}$  are approximated by

$$J_m(x) \approx \sqrt{\frac{2}{\pi}} \frac{1}{\sqrt{x \sin Q}} \cos \left[ x (\sin Q - Q \cos Q) - \frac{\pi}{4} \right], \quad (\text{A1})$$

$$Y_m(x) \approx \sqrt{\frac{2}{\pi}} \frac{1}{\sqrt{x \sin Q}} \sin \left[ x (\sin Q - Q \cos Q) - \frac{\pi}{4} \right], \quad (\text{A2})$$

where  $\cos Q = m/x$ . For  $|m| > k_e R_S + \sqrt[3]{k_e R_S}$  an analogous expansion<sup>34</sup> can be used. In the intermediate range  $|m - k_e R_S| < \sqrt[3]{k_e R_S}$  one may apply uniform asymptotic expansions<sup>34</sup> for the Bessel functions. For Bessel functions of a complex argument  $z$  with fixed  $m$  the approximate form<sup>34</sup>

$$J_m(z) \approx \sqrt{\frac{2}{\pi z}} \cos \left( z - \frac{1}{2} m \pi - \frac{\pi}{4} \right), \quad \text{for } z \rightarrow \infty \quad (\text{A3})$$

will be used. We first calculate the eigenphase  $\Phi_m(\varepsilon)$  for  $|m| < k_e R_S - \sqrt[3]{k_e R_S}$ . Using Eqs. (A1)-(A3) for the Bessel functions in Eqs. (23) and (25), one finds

$$e^{i\Phi_m(\varepsilon)} = \frac{1 + e^{-2i[\vartheta_m(k_e R_N) - \vartheta_m(k_e R_S) + \beta^*]}}{1 + e^{2i[\vartheta_m(k_e R_N) - \vartheta_m(k_e R_S) + \beta]}} e^{2i[\vartheta_m(k_e R_N) - \vartheta_m(k_e R_S)]} e^{i(\beta + \beta^*)}, \quad (\text{A4})$$

where

$$\vartheta_m(x) = \sqrt{x^2 - m^2} - |m| \arccos \frac{|m|}{x}, \quad (\text{A5})$$

$$\beta = q_e R_S - \frac{1}{2} m \pi - \frac{\pi}{4}. \quad (\text{A6})$$

The absolute values of  $m$  in the above expressions are the consequence of degeneracy of the eigenstates  $m$  and  $-m$ . Note that  $\beta$  is a complex number. Thus, for  $\Delta_0 \ll E_F$  and below the gap  $\eta \ll 1$ , Eq. (12) yields

$$\beta = k_F R_S - \frac{1}{2} m \pi - \frac{\pi}{4} + i \frac{R_S}{\xi(\varepsilon)}, \quad (\text{A7})$$

where the coherence length  $\xi(\varepsilon)$  is defined<sup>6</sup> as

$$\xi(\varepsilon) = \frac{\hbar v_F}{\sqrt{\Delta_0^2 - \varepsilon^2}} = \frac{2}{k_F |\eta|}. \quad (\text{A8})$$

Here  $v_F$  is the Fermi velocity. We now assume that  $R_S \gg \xi(\varepsilon)$ . The opposite case will be discussed in Sec. V. Then, the first factor in Eq. (A4) is approximately equal to 1, and we obtain

$$\Phi_m(\varepsilon) = 2 [\vartheta_m(k_e R_N) - \vartheta_m(k_e R_S)] + 2k_F R_S - m\pi - \frac{\pi}{2}. \quad (\text{A9})$$

We now turn to the case  $|m| > k_e R_S + \sqrt[3]{k_e R_S}$ . In this case, according to the analogous Debye asymptotic expansion of the Bessel functions, one finds that  $J_m(k_e R_S)$  can be neglected (it is exponentially small) compared to the second term of the 1,1 element of the determinant in (23). Similarly,  $J'_m(k_e R_S)$  is also negligible in the determinant. Thus, the ratio  $J_m(k_e R_N)/Y_m(k_e R_N)$  can be taken out from the determinant. It turns out that the remaining determinant is not equal to zero for  $\varepsilon < \Delta_0$ . Thus, to a very good approximation,  $D_m^{(e)}(\varepsilon)$  (as a function of  $\varepsilon$ ) has zeros whenever  $J_m(k_e R_N) = 0$ . This corresponds to the energy levels of a circular billiard of radius  $R_N$  for electron-like quasiparticles. Note that now  $\Phi_m(\varepsilon)$  cannot be calculated from Eq. (25), since  $D_m^{(e)}(\varepsilon) \approx 0$  for  $|m| > k_e R_S + \sqrt[3]{k_e R_S}$ . In this case we shall use a different method to determine the contributions to the smooth part of the counting function.

To approximate  $D_m^{(e)}(\varepsilon)$  in the intermediate range  $|m - k_e R_S| < \sqrt[3]{k_e R_S}$ , one may apply uniform asymptotic expansions for Bessel functions. Semiclassically, these states are related to the diffraction of the electron in the penumbra of a circular annulus billiard<sup>35</sup>. As a first estimate of the smooth part of the counting function, the energy levels in the intermediate range will be taken into account by the corresponding energy levels of the circular billiard of radius  $R_N$  using Debye's asymptotic expansion. As we shall see, this is a good approximation since the intermediate range of  $m$  is rather narrow compared to the two other ranges discussed above. Using the uniform expansions of the Bessel functions in our derivation of the Weyl formula for the NS disk system, it is straightforward (although algebraically rather tedious) to include the intermediate range more accurately.

Similarly, the method of approximations outlined above can be used to approximate  $D_m^{(h)}(\varepsilon)$  in the secular equation (19). One finds that  $\Phi_m(-\varepsilon)$  is still given by (A9) after replacing  $k_e$  by the wave number  $k_h(\varepsilon) = k_e(-\varepsilon)$  of the hole-like quasiparticles in the N region. However, in this case the approximation for  $\Phi_m(-\varepsilon)$  is valid only for  $|m| < k_h R_S - \sqrt[3]{k_h R_S}$ . Finally, from Eq. (A9) one obtains

$$\Phi_m(\varepsilon) - \Phi_m(-\varepsilon) = 2 [\vartheta_m(k_e R_N) - \vartheta_m(k_e R_S)] - 2 [\vartheta_m(k_h R_N) - \vartheta_m(k_h R_S)] \quad (\text{A10})$$

for  $|m| < k_h R_S - \sqrt[3]{k_h R_S}$ . Note that the last three terms in (A9) cancel out in the difference  $\Phi_m(\varepsilon) - \Phi_m(-\varepsilon)$ .

In a similar way, it can be seen that the zeros of  $D_m^{(h)}(\varepsilon)$  in Eq. (19) coincide with the zeros of  $J_m(k_h R_N)$  for  $|m| > k_h R_S + \sqrt[3]{k_h R_S}$  to a good approximation. Thus, the secular equation (19), determining the energy levels of the NS disk system, reduces to

$$J_m(k_e R_N) J_m(k_h R_N) = 0 \quad (\text{A11})$$

for  $|m| > k_e R_S + \sqrt[3]{k_e R_S}$ . The energy levels are the same as those of the disk of radius  $R_N$  for electron/hole-like quasiparticles. Semiclassically, the states with angular momentum quantum number  $|m| > k_e R_S + \sqrt[3]{k_e R_S}$  are called whispering gallery modes. The wave functions for these states at  $r = R_S$  are negligible, and so no Andreev reflections take place. This is why the superconducting pair potential  $\Delta_0$  does not appear in (A11).

<sup>1</sup> A. F. Andreev, Zh. Eksp. Teor. Fiz. **46**, 1823 (1964), [Sov. Phys. JETP, **19**, 1228 (1964)].

<sup>2</sup> C. J. Lambert and R. Raimondi, J. Phys. Condens. Matter **10**, 901 (1998).

<sup>3</sup> C. W. J. Beenakker, in *Mesoscopic Physics, Les Houches Summer School*, edited by E. Akkermans, G. Montambaux, J. L. Pichard, and J. Zinn-Justin (Elsevier Science B. V., Amsterdam, 1995).

<sup>4</sup> *Mesoscopic Electron Transport*, edited by L. L. Sohn, L. P. Kouwenhoven, and G. Schön (Kluwer Academic Publishers, Dordrecht, The Netherlands, 1996).

<sup>5</sup> C. W. J. Beenakker, Rev. Mod. Phys. **69**, 731 (1997).

<sup>6</sup> P. G. de Gennes, *Superconductivity of Metals and Alloys* (Benjamin, New York, 1996).

<sup>7</sup> P. G. de Gennes and D. Saint-James, Phys. Lett. **4**, 151 (1963).

<sup>8</sup> I. Kosztin, D. L. Maslov, and P. M. Goldbart, Phys. Rev. Lett. **75**, 1735 (1995).

- <sup>9</sup> J. A. Melsen, P. W. Brouwer, K. M. Frahm, and C. W. J. Beenakker, *Eur. Phys. Lett.* **35**, 7 (1996)
- <sup>10</sup> J. A. Melsen, P. W. Brouwer, K. M. Frahm, and C. W. J. Beenakker, *Physica Scripta* **T69**, 223 (1997).
- <sup>11</sup> A. Altland and M. R. Zirnbauer, *Phys. Rev. Lett.* **76**, 3420 (1996).
- <sup>12</sup> G. B. Lesovik, A. L. Fauchère, and G. Blatter, *Phys. Rev. B* **55**, 3146 (1997).
- <sup>13</sup> A. Lodder and Y. V. Nazarov, *Phys. Rev. B* **58**, 5783 (1998).
- <sup>14</sup> H. Schomerus and C. W. J. Beenakker, *Phys. Rev. Lett.* **82**, 2951 (1999).
- <sup>15</sup> W. Ihra, M. Leadbeater, J. L. Vega, and K. Richter, *Eur. Phys. J. B* **21**, 425 (2001).
- <sup>16</sup> I. O. Kulik, *Zh. Éksp. Teor. Fiz.* **57**, 1745 (1969), [*Sov. Phys. JETP* **30**, 944 (1970)]; J. Bardeen and J. L. Johnson, *Phys. Rev. B* **5**, 72 (1972).
- <sup>17</sup> C. W. J. Beenakker, *Phys. Rev. Lett.* **67**, 3836 (1991), [**68**, 1442, (1992) (Erratum)]; C. W. J. Beenakker, in *Transport Phenomena in Mesoscopic Systems*, edited by H. Fukuyama and T. Ando (Springer-Verlag, Berlin, 1992), pp. 235–253.
- <sup>18</sup> P. F. Bagwell, *Phys. Rev. B* **46**, 12573 (1992).
- <sup>19</sup> H. Hoppe, U. Zülicke, and G. Schön, *Phys. Rev. Lett.* **84**, 1804 (2000).
- <sup>20</sup> O. Šipr and B. L. Györfy, *J. Phys.: Condens. Matter* **8**, 169 (1996); O. Šipr and B. L. Györfy, *J. Low. Temp. Phys.* **106**, 315 (1997).
- <sup>21</sup> H. Weyl, *Nachr. Akad. Wiss.* 110 (1911).
- <sup>22</sup> M. Brack and R. K. Bhaduri, in *Semiclassical Physics*, edited by D. Pines (Addison-Wesley Pub. Co., Inc., Amsterdam, 1997).
- <sup>23</sup> C. Bruder and Y. Imry, *Phys. Rev. Lett.* **80**, 5782 (1998).
- <sup>24</sup> P. Visani, A. C. Mota, and A. Pollini, *Phys. Rev. Lett.* **65**, 1514 (1990); A. C. Mota, P. Visani, A. Pollini, and K. Aupke, *Physica (Amsterdam)* **197B**, 95 (1994); A. C. Mota, P. Visani, A. Pollini, and K. Aupke, *Physica (Amsterdam)* **197B**, 95 (1994); F. B. Müller-Allinger and A. C. Mota, *Phys. Rev. Lett.* **84**, 3161 (2000).
- <sup>25</sup> G. E. Blonder, M. Tinkham, and T. M. Klapwijk, *Phys. Rev. B* **25**, 4515 (1982).
- <sup>26</sup> W. L. McMillan, *Phys. Rev.* **175**, 559 (1968); G. Kieselmann, *Phys. Rev. B* **35**, 6762 (1987).
- <sup>27</sup> H. Plehn, O.-J. Wacker and R. Kümmel, *Phys. Rev. B* **49**, 12140 (1994).
- <sup>28</sup> Y. Asano and T. Kato, *J. Phys. Soc. Jpn.* **69**, 1125 (2000).
- <sup>29</sup> E. Doron and U. Smilansky, *Phys. Rev. Lett.* **68**, 1255 (1992).
- <sup>30</sup> U. Smilansky, in *Mesoscopic Quantum Physics, Les Houches Summer School*, edited by E. Akkermans, G. Montambaux, J. L. Pichard, and J. Zinn-Justin (Elsevier Science B. V., Amsterdam, The Netherlands, 1995).
- <sup>31</sup> M. Berry, in *Chaos and Quantum Physics, Les Houches Summer School*, edited by M.-J. Giannoni, A. Voros, and J. Zinn-Justin (Elsevier Science B. V., Amsterdam, The Netherlands, 1991).
- <sup>32</sup> Z. Kaufmann, (unpublished).
- <sup>33</sup> N. A. Mortensen, K. Flensberg, and A.-P. Jauho, *Phys. Rev. B* **59**, 10176 (1999).
- <sup>34</sup> M. Abramowitz and I. Stegun, *Handbook of Mathematical Functions*, 9th ed. (Dover Publication Inc., New York, NY, 1972).
- <sup>35</sup> H. Primack, H. Schanz, U. Smilansky, and I. Ussishkin, *Phys. Rev. Lett.* **76**, 1615 (1996); N. C. Snaith and D. A. Goodings, *Phys. Rev. E* **55**, 5212 (1997).